

DEVELOPMENT OF NEW TECHNIQUES FOR TELOMERE LENGTH ANALYSIS
IN AGING YEAST CELLS AND IN SENESCENT CELLS RESCUED BY
REACTIVATION OF TELOMERASE

THESIS

Presented to the Graduate Council of
Texas State University-San Marcos
in Partial Fulfillment
of the Requirements

for the Degree
Master of SCIENCE
by

Christopher K. Lee, B.S.

San Marcos, Texas
December 2009

ACKNOWLEDGEMENTS

Foremost, this thesis project would not have been possible without my advisor, Dr. Lewis. Thank you for having confidence in my abilities and for granting me a fascinating research project. Through your guidance, I was able to overcome challenges along the way. You are not only an exceptional professor, but one of the most compassionate individuals I have ever met. Your mentoring and exemplary character has left an enduring impression on me.

I tremendously appreciate Dr. Booth and Dr. David for serving on my thesis committee and for providing professional feedback to improve the quality of my thesis. Throughout each semester, I was fortunate to have worked alongside supportive labmates and friends, including Mike Robson and Sunaina Sethi. Overall, being a graduate student and teaching assistant, I gained a wealth of scientific knowledge and many personal memories. I am proud to be a part of Texas State University-San Marcos.

I owe my success to the Heavenly Father, for His countless blessings in my life. To my parents, I love you both and hope to honor you with my thesis. Also, I wish to thank my Uncle John for the countless advice and support you have given me. Finally, to my darling Erika, thank you for your encouragement while I worked persistently to complete my thesis. You are an amazing individual, and have a bright future ahead.

TABLE OF CONTENTS

	Page
ACKNOWLEDGEMENTS.....	iii
LIST OF TABLES.....	v
LIST OF FIGURES	vi
CHAPTER	
I. INTRODUCTION	1
II. MATERIALS AND METHODS.....	12
III. RESULTS AND DISCUSSION.....	23
REFERENCES	61

LIST OF TABLES

Table	Page
1. Calculated fragment sizes (bp) of the lower band observed in Southern blots used to evaluate telomere length after multiple generations in telomerase-deficient cells.....	54
2. Calculated fragment sizes (bp) of the lower band observed in Southern blots used to evaluate telomere length restoration in telomerase reactivated (<i>EST2</i>) cells.....	57

LIST OF FIGURES

Figure	Page
1. Illustration showing the basic components of a eukaryotic chromosome	5
2. Illustration of the analogy between the telomerase complex in <i>S. cerevisiae</i> and humans	7
3. Schematic depiction of telomere shortening and protein uncapping processes.....	24
4. Illustration of the Est2 polymerase expression system indicating the activation (galactose media) or deactivation (glucose media) of telomerase	26
5. Column streaks of mutant <i>est2</i> cells grown on synthetic glucose plates	27
6. Illustration of PCR labeling of digoxigenin (DIG) labeled dUTP to generate a DNA probe for Southern blot experiments.....	28
7. Illustration of the immunochemical detection method for Southern blot experiments	29
8. Confirmation of the synthesis of a DIG-labeled probe on a 3% agarose gel	30
9. Digested yeast chromosomal DNA visualized on an agarose gel and subsequent assay by Southern blotting, visualized on x-ray film	31
10. The Southern blot technique	32
11. Southern blot detection of <i>S. cerevisiae</i> chromosome ends.....	33
12. Southern blot performed to resolve upper (high molecular weight) bands in the top portion of the gels.....	34

13. Standard curve for telomere length quantitation.....	35
14. Example illustrating the differences in band size, as seen in Southern blots	36
15. Telomere bands detected experimentally compared to the projected band pattern of XhoI digested, BY4742 (wildtype) DNA	38
16. Assignment of chromosome ends to Southern blot bands.....	40
17. Average DNA concentrations of yeast chromosomal DNA purified using 3% SDS cell lysis solutions, with or without 0.2 M NaOH, and a 65 °C incubation period.....	43
18. Average DNA concentrations after different protein precipitation reagents were used for DNA purification.....	44
19. Agarose gel electrophoresis of purified DNA samples each using a different alkali precipitation reagent	45
20. Average concentrations of yeast chromosomal DNA purified purified using different concentrations of SDS	46
21. Average DNA yields quantified from purifications performed using 6% SDS solutions with and without increasing concentrations of Tris buffer.....	47
22. Average DNA concentration of samples purified using cell lysis reagents with 30 mM Tris buffer and variable SDS concentrations	48
23. A 0.6% agarose gel showing fluorescent bands of yeast chromosomal DNA purified using variable SDS concentrations with Tris.....	49
24. Comparison of average DNA concentrations of purified product using the SDS method versus a commercial kit for yeast chromosomal DNA purification	50

25. Agarose gel electrophoresis to compare relative DNA concentrations based on differential fluorescent band intensity	51
26. A 0.6% agarose gel separating fragments of yeast chromosomal DNA digested with EcoRI following purification using three different sets of reagents.....	52
27. Southern blot analysis of telomere fragment lengths after XhoI digestion of YLKL803 (<i>est2</i>) chromosomal DNA	54
28. Southern blot analysis of post-senescent telomere length maintenance of YLKL803 cells rescued by (<i>EST2</i>) telomerase reactivation	57

CHAPTER I

INTRODUCTION

The average human life expectancy has increased dramatically over the years with advancements in medical technology and improved sanitation; however maximum human lifespan still remains at about 120 years. This upper boundary of life indicates an inherent mechanism for cellular replicative capacity which can only be elucidated on the molecular level. Cellular aging is becoming an area of increasing interest for scientific research given the prominence and mortality of age-related diseases including cardiovascular disease and cancer. It is of interest and benefit to society to develop practical applications from this research in the form of preventative therapy.

A decreasing proportion of proliferative cells over time *in vitro* is one parameter that can be used to assess aging (1). In contrast to the germline and certain stem cells, most human somatic cells grown in culture undergo a finite number of cell divisions and then terminally cease to divide. These post-mitotic cells are under permanent growth arrest, a state termed cellular senescence. The finite replicative lifespan of normal cells *in vitro* was first observed approximately 50 years ago and termed the Hayflick limit (2). In addition to functional deficiencies, senescent cells display significant alterations in mass and morphology in contrast to proliferating cells (3). Scientific evidence strongly

suggests that senescence does in fact occur *in vivo* and is implicated in important processes such as tumor suppression, vascular diseases, and aging (2, 4).

Cells are aggregates of macromolecules and the fundamental structural and functional units of all living things. They can be divided into two basic classifications: prokaryotic and eukaryotic. Prokaryotic cells are represented by archaea and bacteria which are relatively simple yet highly successful single-celled life forms. Eukaryotic cells constitute higher organisms, which range from complex multicellular plants and animals to unicellular and simple multicellular protozoans, fungi and algae. Eukaryotes typically have larger cell sizes than prokaryotes and contain membrane-enclosed organelles for specialized cellular functions. The principal feature that distinguishes these two general classes of organisms is the presence or absence of a membrane-bound nucleus (5).

The nucleus houses most of the cell's genetic material and is a distinct structure segregated from the rest of the cell by a selectively permeable nuclear envelope. This membrane is a lipid bilayer perforated with nuclear pore complexes that govern the transportation of cell components into or outside the nucleus (6). The genetic information of all living organisms is universally encoded in the form of DNA (deoxyribonucleic acid) and is stored within the cell nucleus as compact structures called chromosomes. The eukaryotic genome is divided into multiple chromosomes, each containing a single long, linear DNA molecule coiled around histone proteins. Most prokaryotes have a single circular chromosome and are haploid, because they carry only one complete chromosome copy. Eukaryotes are predominantly composed of diploid

cells that contain two identical copies of every chromosome with the exception of haploid sex cells (sperm and eggs) involved in reproduction (7).

Chromosomes by weight consist of approximately equal amounts of histones, non-histone proteins, and DNA. DNA is a type of nucleic acid consisting of polymeric chains of covalently-linked nucleotide monomers that form a double helix configuration. Each monomer unit contains a single five-carbon sugar, deoxyribose, which is distinguishable from RNA by the absence of a hydroxyl group at the 2' carbon position. These successive sugar residues are connected via a phosphate group attached to a 5' end of one and to the 3' end of the adjoining nucleotide. Collectively, this repeated phosphodiester linkage constructs the nucleic acid backbone and is the exterior of the helix (5, 8).

Each deoxyribose monomer in the chain carries one of two types of heterocyclic nitrogenous bases, a purine or pyrimidine, attached to the 1' carbon through a glycosidic bond. There are four different bases in DNA: two purines, adenine (A) and guanine (G) and two pyrimidines, cytosine (C) and thymine (T). RNA contains the same bases except that uracil (U) replaces thymine. The double strands of DNA are held together, in part, through a vast accumulation of hydrogen-bonding interactions arranged inside the helix. These bonds are formed between nucleotides and confer specificity in standard Watson-Crick base pairing where A pairs with T, and G pairs with C. Although both strands share the same helical geometry, they are antiparallel in chemical polarity as a stereochemical consequence of complementary base pairing. The double helix secondary structure also permits sharing of pi electrons between aromatic rings of adjacent

nucleotide bases. This electrostatic interaction within the helix is known as base stacking and further stabilizes the duplex polymer (5, 8).

Regions of DNA that control discreet hereditary characteristics are known as genes and each usually corresponds to a single protein or functional RNA molecule. Cells convert the nucleotide sequence of genes into the amino acid sequence of proteins through the process of gene expression (8). Typically, the greater an organism's apparent complexity, the larger its genome and the number of genes it possesses. The gene density of eukaryotic genomes however, is lower and more variable than those of prokaryotes. This decreased gene density is attributed to greater amounts of non-coding, intergenic sequences and repetitive sequences. Within the protein coding regions are non-expressed sequences called introns that require splicing after messenger RNA transcription (7).

Besides carrying genes, eukaryotic chromosomes possess three different DNA elements critical for genomic stability: two telomeres, a centromere, and many origins of replication (Figure 1) (7). The centromere is a region which adheres sister chromatids and serves as the attachment site for a mitotic spindle during cell division (9, 10). In complex eukaryotes, centromeres are usually composed of highly repetitive satellite sequences that are minimally hundreds of kilobases in size (10). A protein complex referred to as the kinetochore is directed to and assembled upon this region. Kinetochores interact with both centromere DNA and mitotic spindles to pull sister chromosomes toward opposite microtubule-organizing centers during cell division (7, 9). It is important that only one centromere is present and functional on each chromosome. Chromosome malsegregation produces aneuploid cells, a potentially lethal outcome for the cell (11).

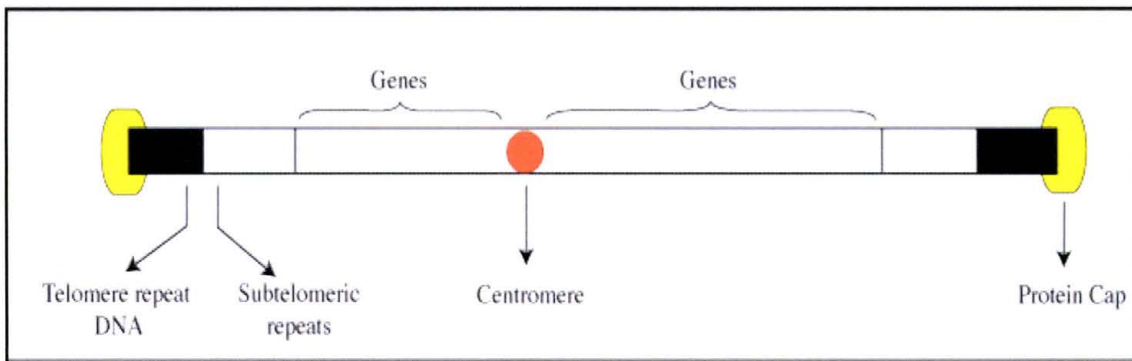


Figure 1. Illustration showing the basic components of a eukaryotic chromosome.

Another sequence element is the telomere, which is a specialized DNA-protein structure located at the physical ends of linear chromosomes. Telomeres consist of highly conserved, long arrays of G-rich tandemly repeated DNA sequences that end with a 3' single-stranded DNA (ssDNA) overhang. In humans, the repeat sequence tract is $(TTAGGG)_n$ and is typically 8-12 kb in length at birth (12). Tract length varies among different telomeres within an individual cell as well as at the same telomere in different cells. Immediately adjacent to the telomeres are the subtelomeric regions. Subtelomeres consist of stretches of low copy, segmentally duplicated DNA tracts with high sequence similarity between the tracts (13). Human telomeres may adopt intramolecular G-quadruplex structures stabilized by stacking of G tetrads from Hoogsteen G-G pairing (14). The ssDNA overhang can base-pair with internal telomere repeats, forming a lasso-like structure known as a telomere loop (t loop) and a single-stranded displacement loop (D loop) at the invasion site (12). Furthermore, the telomere region is capped with a complex of sequence-specific DNA-binding proteins essential for telomere maintenance and chromosome stability (15).

During semi-conservative DNA replication, telomeric DNA is progressively lost at chromosome ends following each cell division. Due to the requirement for a 5' RNA primer on the lagging strand, conventional DNA polymerases are incapable of complete end-replication. Cells compensate for this deficiency by recruiting telomerase.

Telomerase is a ribonucleoprotein DNA polymerase with an RNA component that serves as a template for telomere synthesis. Through reverse transcription, G-rich telomeric repeats are restored to elongate the 3' terminus during S phase of the cell cycle. This provides additional template to accommodate binding of a final primer for complete strand synthesis (16).

Telomerase of the budding yeast *Saccharomyces cerevisiae* has been well characterized and is analogous to human telomerase (7). Yeast telomerase is a multi-subunit enzyme consisting of the proteins Est1, Est2, Est3 (Ever Shorter Telomeres), Cdc13 (Cell Division Cycle) as well as the RNA subunit *TLC1* (Telomerase Component 1) (Figure 2). Est3 is a component of unknown function. Cdc13 is a single-stranded DNA-binding protein that binds the G-rich overhang and interacts with Est1 to recruit telomerase. Est2 (TERT in mammals) is the catalytic reverse transcriptase and *TLC1* (TR in mammals) encodes the RNA template (17, 18).

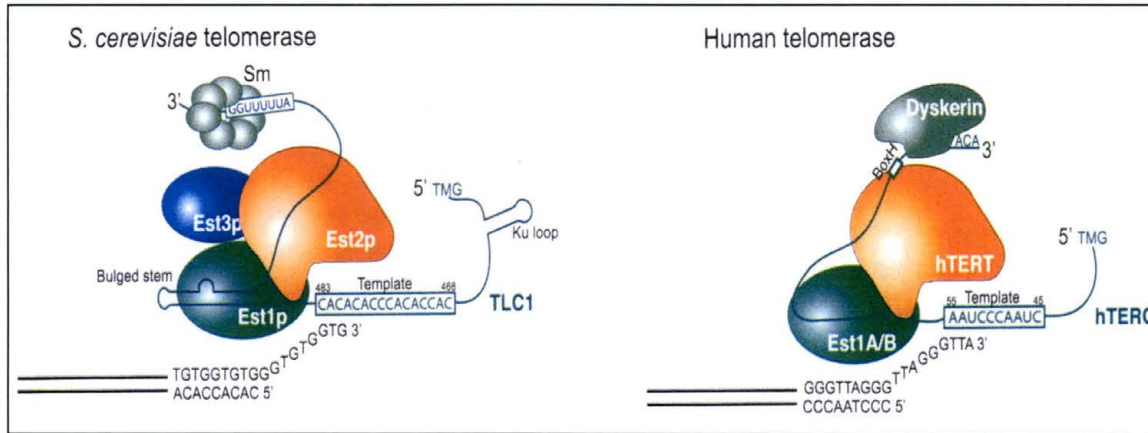


Figure 2. Illustration of the analogy between the telomerase complex in *S. cerevisiae* and humans (7).

Telomerase maintains the telomeres at an optimal length required for genome stability; however, levels of telomerase expression are low or undetectable in most human somatic tissues (12, 19). Consequently, a total lifetime loss of several thousand base pairs in telomere length has been observed in humans (12). The rate of telomere shortening ranges from 40-200 bp per cell division, depending on cell type (20). In *S. cerevisiae*, inactivation of telomerase results in progressive telomere attrition followed by loss of growth potential, chromosome instability, and eventual cell death. Telomere dysfunction is attributed to ssDNA generation and disruption of telomere-binding proteins (15, 21, 22). Uncapped chromosomes are inadvertently detected by the cell as double-stranded DNA breaks (DSBs), which are not tolerated and undergo rapid repair (15, 22). This loss of end protection activates a DNA damage checkpoint response and G₂/M phase cell-cycle arrest (15). Unprotected chromosome ends may be susceptible to end resection or aberrant end-to-end fusions through non-homologous end-joining (NHEJ) or homologous recombination (HR) (12, 18, 21).

In humans, telomerase is active in stem cells and the germ line, but most normal somatic cells have low or undetectable enzyme activity (23). Without telomere maintenance, cells experience progressive telomere shortening. As in yeast cells (described above), once telomere degradation reaches a critically short level, the t loop becomes disrupted and uncapped, triggering cell-cycle arrest (24, 25).

Relicative senescence was first reported in human diploid fibroblasts (HDFs) which were discovered to divide for approximately 50 generations in culture and then indefinitely arrest growth (12). Senescent cells adopt an altered morphology and possess multiple differences in cellular physiology compared to normal cells (27). Based on this phenotype, studies have identified senescent cells *in vivo*. For example, an accumulation of senescent cells in aging human skin and liver reportedly has been detected. It is therefore believed that cellular senescence is closely related to the degenerative changes associated with whole organismal aging (26).

Genetic instability as a result of telomere dysfunction is a powerful mutagen that facilitates tumor formation. Most cancer cells circumvent senescence and immortalize by turning telomerase expression back on (21, 28). This is perceived to be a major mechanism underlying carcinogenesis, considering that 90% of human tumor cell lines express high levels of telomerase (27, 28, 29). Unlimited replicative potential conferred by telomerase activity may also increase the likelihood for mutation of the p53 tumor suppressor gene, an event frequently detected in human cancer (29).

Senescence of yeast cells can be modeled *in vitro*, detected by declining numbers of colony-forming units with decreased colony sizes on Petri dishes due to cell cycle delays (30). As telomeres reach critically short levels in telomerase-deficient yeast cells,

replicative potential declines and cells arrested in the G₂/M phase of the cell cycle accumulate (15, 24). In rare instances, these cells can escape senescence by acquiring a mutation that stimulates recombination-dependent mechanisms to amplify telomeric and subtelomeric repeats (31). Since telomere stability is correlated with cell viability and age, telomere length in humans is becoming a predictive indicator for disease risk and premature mortality (2).

The relatively simple unicellular eukaryote *S. cerevisiae* is an advantageous experimental model system for in-depth studies of cellular aging (32). It is a favored model owing to its relatively small genome size and small number of genes, of which many are conserved in humans. Also, it can grow in either a haploid or diploid state, mediated by cell mating and sporulation. The complete genomic sequence of *S. cerevisiae* was published in 1996, the first for any eukaryote (7). Importantly, it is easily grown in the lab with a relatively short generation time (90 min for a wild type strain at 30 °C) with low susceptibility to contamination. Many mutant strains have been identified in budding yeast for genes encoding factors involved in a wide array of cellular functions (28). Due to its high rate of homologous recombination, transformation can be more efficiently performed to manipulate the genome than is possible for most other model organisms. This allows researchers to delete and mutate specific genes, as well as replace their upstream regulatory elements. Additionally, yeasts reproduce by budding, and as they progress through the cell cycle, they undergo characteristic changes in morphology that provide valuable information regarding cellular status (7).

Different models have been proposed to explain the genomic instability associated with cellular senescence. One such model is that reactive, uncapped telomere ends elicit

chromosome rearrangements such as end-to-end chromosome fusions (15, 33). Fused chromosomes are dicentrics and would lead to anaphase bridges and chromosome breakage during mitosis, a potentially lethal consequence if essential genes are lost (33). Another suggested chromosomal rearrangement is end resection generated by 5' exonucleolytic degradation (15, 21, 23). In response to dysfunctional telomeres, mammalian cells can activate a checkpoint response that theoretically might result in apoptosis (programmed cell death) through p53-dependent pathways (12, 16). An alternative, non-lethal fate is that cells indefinitely arrest growth in the G₂ phase but remain viable for a prolonged period of time before actual death. Possessing no fatally disarrayed chromosomes or cell-death commitment, they would simply be unable to divide as a result of activated checkpoint proteins and repair pathways (23, 33).

One focus of the Lewis laboratory is the investigation of molecular processes involved in cell aging by modulating telomerase expression in budding yeast. Experimental results from the thesis project of Sandra Bacerra, a former graduate student of the Lewis lab, refuted the aforementioned models of senescence involving lethal cell outcomes. The latter model was supported by demonstrating that senescent cells remain viable for several days, capable of being rescued by simple reactivation of telomerase (34). It was not determined, however, whether or not telomerase expression resulted in telomere restoration to wildtype lengths.

A major aim of the current thesis project was to evaluate telomere length restoration in senescent cells rescued by reactivation of telomerase. Also, for the first time, all 32 chromosome ends of *S. cerevisiae* DNA seen in Southern blot experiments were characterized, based on published telomere and subtelomere DNA sequences. This

improved method of Southern blot analysis can be used to quantitate the loss of telomere DNA at chromosome ends during senescence and also to measure telomere changes following senescence resulting from reactivation of telomerase.

In order to perform Southern blots, as well as many other molecular techniques, it is first necessary to isolate chromosomal DNA from the organism. Yeasts present challenges to purification due to the presence of a complex cell wall and are often resistant to traditional methods used to isolate DNA from other organisms. Previous methods of yeast chromosomal DNA purification have often involved use of enzyme preparations of zymolyase or lyticase to degrade the cell walls (36). These approaches can be tedious and expensive when purifying DNA in large quantities. Cell wall and cell membrane disruption has also been performed by vortexing with glass beads. However, this results in the release of smaller DNA fragments due to mechanical shearing of high molecular weight DNA (37, 38). One chemical-based protocol achieved disruption by repeated freezing and thawing of cells followed by DNA extraction with a chloroform-phenol mixture (37).

The second objective of this project was to develop a new chemical-based method for purifying yeast genomic DNA. Chemical-based purifications are simpler to use than enzymatic-based methods and circumvent DNA shearing caused by glass beads. However, there are limited protocols available and dependence remains high on expensive commercial purification kits whose contents are unknown. The approach that was developed is simpler than other published protocols and requires only common laboratory chemicals.

CHAPTER II

MATERIALS AND METHODS

I. MATERIALS

General reagents

Sodium chloride and sodium citrate dihydrate were purchased from Fisher Scientific (Fair Lawn, NJ). Agarose, Tween 20 and Sarkosyl (N-lauryl-sarcosine) were obtained from Sigma-Aldrich Chemical Co. (St. Louis, MO). Sodium hydroxide was purchased from EM Science (Darmstadt, Germany). Sodium acetate and sodium dodecyl sulfate were purchased from Mallinckrodt Baker, Inc. (Paris, KY). TRIS base was purchased from VWR International (West Chester, PA). Ethidium bromide was purchased from Shelton Scientific (Shelton, CT). Ethylenediaminetetraacetic acid (EDTA) and boric acid were purchased from EM Science (Gibbstown, NJ). Formamide was obtained from Mallinckrodt Chemicals (Phillipsburg, NJ). TE buffer and RNase A were obtained from Epicentre Biotechnologies (Madison, WI). Reagents purchased for Southern blot analysis include: DIG Wash and Block Buffer Set (including 10x blocking agent, 10x maleic acid buffer, 10x detection buffer and 10x washing buffer), DIG High Prime DNA Labeling and Detection Starter Kit II (including blocking agent, DIG easy hyb granules and CSPD), anti-digoxigenin-AP Fab fragments, PCR DIG labeling mix

and DNA Molecular Weight Marker III – Dig Labeled were obtained from Roche Diagnostics (Indianapolis, IN).

Bacteriological and yeast growth media

All amino acids, D-(+)-galactose and ampicillin were purchased from Sigma-Aldrich Chemical Co. (St. Louis, MO). Bacto peptone, bacto yeast extract and bacto agar were obtained from Becton Dickinson and Co. Microbiological Systems (Sparks, MD). Anhydrous D-glucose (dextrose) was purchased from Mallinckrodt (Paris, KY).

Enzymes and PCR reagents

Restriction enzymes XhoI and EcoRI, Standard Taq Reaction Buffer and DNA Taq polymerase were purchased from New England Biolabs (Beverly, MA). MgCl₂ (25mM) was purchased from Fermentas, Inc. (Glen Burnie, MD).

Cell culture solutions and media

Yeast cells were grown on YPDA (rich) media (1% bacto yeast extract, 2% bacto peptone, 2% dextrose, 2% bacto agar and 0.002% adenine) for general, nonselective growth. For plasmid selection, yeast cells were grown on synthetic media with drop-out mix (2% glucose or 2% galactose and 2% bacto agar, plus all essential amino acids and bases exempting those used for plasmid selection). Synthetic media plates for senescence assays used 2% glucose, 2% bacto agar and all the essential amino acids and bases exempting those required for plasmid selection. Senescence reactivation experiments required synthetic media plates using 2% glucose or 2% galactose growth media.

YPGalactose used in the reactivation rescue of cells included 1% bacto yeast extract, 2% bacto peptone, 2% bacto agar and 2% galactose respectively. All quantities listed here as “%” are w/v.

Yeast strains and plasmids

The parent strains used for these studies were derived from BY4742 (*MAT α* *his3Δ1 leu2Δ0 lys2Δ0 ura3Δ0*). The *est2* strain utilized in all initial assays was YLKL803 (BY4742, $\Delta est2::HygB'$ containing plasmid pLKL82Y [*CEN/ARS URA3 GAL1-V10p::EST2*]). Reactivation experiment strains included YLKL803 ($\Delta rad52::G418'$). Analysis of telomere lengths using Southern blot assays required the use of a probe prepared by PCR from the plasmid YTCA-1 (39).

SDS/EDTA method for yeast chromosomal DNA purification

For each DNA purification experiment, yeast cells of the lab strain BY4742 were grown using either solid or liquid YPDA media in the following manner. For solid media, a lawn of cells was spread onto 3 YPDA plates and then grown for 2-3 days at 30 °C. To harvest the cell cultures, 7 ml of sterile ddH₂O was transferred to a single plate using a pipet. To thoroughly remove and suspend the cells, a sterile “hockey stick” plate spreader was swept bidirectionally across the agar surface while continuously rotating the plate on a Petri dish turntable. The cell suspension was collected with a 5 ml pipet, transferred to a second cell lawn and the previous steps were repeated. After harvesting the final plate, the cell suspension was transferred to a 15 ml centrifuge tube and pelleted

by 5 min of centrifugation at ~3,500 RPM using a Beckman Coulter Allegra 6 benchtop centrifuge. The resulting supernatant liquid was discarded.

Alternatively, BY4742 cells were also grown in liquid media according to the following steps. First, 1 ml of YPDA broth in a 1.5 ml microfuge tube was inoculated from a wide swath of cells scraped from a stock plate using a sterile toothpick. The cell suspension was vortexed briefly and then transferred to 50 ml of YPDA liquid media in a 250 ml Erlenmeyer flask. Cells in this flask were grown overnight at 30 °C using a Barnstead Max Q 4000 benchtop shaker. On the following day, 1.5 ml aliquots of the liquid culture were transferred to 2.0 ml microcentrifuge tubes and then spun at 16,100 x g for 0.5 min using an Eppendorf 5415 D microcentrifuge. The resulting supernatant liquid was removed and an additional 1.5 ml aliquot of the liquid culture was added to each sample. They were then spun as before to pellet the cells and remove the supernatant.

To begin DNA purification, 300 µl of a cell lysis solution containing specific dilutions of 20% SDS (w/v) and 0.5 M EDTA (some experiments also included aliquots from 5 M NaOH and 1 M Tris, pH 8.0) was added to the cells. The pellets were suspended by repeated pipeting using a P-1000 pipetor and brief vortexing. The cell solutions were then incubated (some experiments included heat as an experimental variable) at 65 °C for 15 min. Each sample then received 150 µl of 3 M KOAc (60% 5 M potassium acetate, 11.5% glacial acetic acid and 28.5% ddH₂O). After a strong 10 sec vortex, the samples were centrifuged at 16,100 x g for 15 min and the supernatant was transferred to a 1.5 ml microfuge tube. To the supernatant, 500 µl of isopropanol was added and the tube was mixed thoroughly by inversion. The solution was centrifuged for

10 min and the supernatant was removed and discarded. Next, the DNA pellets were washed with 500 µl 70% ethanol for 1 min, which was then removed with a P-200. To dry the pellets, samples were spun in a Savant Speed Vac for 10 min with vacuum and medium heat applied. Fifty µl of TE was added to each sample to suspend the DNA followed by 1 µl of 1 mg/ml RNase A (some experiments included RNase A as an experimental variable and it was excluded for some samples). The tubes were gently vortexed and placed in a 37 °C waterbath to incubate for 30 min and then stored at 4 °C overnight. On the following day, the purified DNA samples were centrifuged for 2 min and the solutions were transferred to new 1.5 ml microfuge tubes to remove any insoluble substances. After usage, samples were stored at -20 °C for preservation.

Fluorometry assay

After the purified DNA had undergone RNase treatment, the DNA concentrations were quantified using a Hoefer DyNA Quant 200 Fluorometer (Amersham Pharmacia Biotech). The protocol required the use of standard calf thymus DNA (100 µg/ml) for calibration and assay solution A (0.1 µg/ml Hoechst 33258 and 1x TNE [0.2 M NaCl, 10 mM Tris-HCl and 1 mM EDTA at pH 7.4]).

Protocol: SDS/EDTA method for yeast chromosomal DNA purification

The optimum protocol for extraction of yeast chromosomal DNA that was developed based on these experiments is as follows:

1. Start a 4 ml culture of yeast cells and shake overnight at 30 °C. (Alternatively,

- spread or patch yeast cells to the surface of a plate and grow at 30 °C for ~ 2 days)
2. Transfer 1.5 ml of the culture to a microfuge tube, spin at full speed in a microcentrifuge for 0.5 min, pour off supernatant, add 1.5 ml more cells to the tube, re-spin for 0.5 min and pour off supernatant again. Add 300 µl SET (SDS + EDTA + Tris) solution* and scrape the tube across the bottom of a test tube rack several times to resuspend the cells.

Note: If cells are to be harvested from a long patch on a plate, use a toothpick to scrape cells directly into 300 µl of 6% SET solution. If using a lawn of cells that was spread onto a plate surface, add 7 ml sterile ddH₂O to the lawn, use a sterile glass hockey stick to evenly spread the liquid and suspend the cells, pipet into a 15 ml screw cap tube, spin in table top centrifuge for 5 min, remove supernatant, resuspend in 300 µl SET solution and transfer to a 1.5 ml tube.
 3. Incubate the suspended cells at 65 °C for 15 min and then transfer to wet ice for 5 min.
 4. Add 150 µl cold 3 M KOAc alkaline lysis solution**. Vortex for 10 sec.
 5. Spin in microfuge 15 min at full speed. Transfer the supernatant to a 1.5 ml tube.
 6. Add 500 µl isopropanol and mix thoroughly by inverting vigorously.
 7. Spin 10 min at full speed and remove the supernatant.
 8. Wash DNA pellet by adding 500 µl of cold 70% EtOH. Wait 1 min and remove with a P-200.
 9. Dry in speedvac for 10 min on low heat.
 10. Suspend DNA pellet in 50 µl TE.

11. Add 1 µl RNase A. Vortex gently and incubate at 37 °C for ~15 min.
12. Allow DNA to dissolve at 4 °C. Occasionally insoluble material is visible in the TE later. Remove it by spinning for 3 min and transferring DNA to a new microfuge tube.

*6% SET solution: (5 ml)

1500 µl 20% SDS (6% final)

100 µl 0.5 M EDTA (10 mM final)

150 µl 1 M Tris (pH 8.0)

3250 µl ddH₂O

**KOAc alkaline lysis solution: (50 ml)

30.0 ml 5 M KOAc (3 M final)

5.75 ml glacial acetic acid (2 M final)

4.25 ml ddH₂O

Solid media-based senescence assays

In vitro cell senescence was observed by streaking double-columns of telomerase-deficient (*est2*) and wildtype control cells (BY4742) onto synthetic glucose minus uracil (glu-ura) plates. This was done by first picking a swath of individual colonies from the low colony density regions of a recently streaked gal-ura stock plate using sterile toothpicks. The cells were grown for three days at 30 °C and then re-streaked from 2-3 moderate-sized individual colonies onto a fresh glu-com plate again. This process was repeated through 4 streaks with the cells growing for approximately 20 generations on each of the first three plates. The assay was discontinued after the fourth streak because of the prominence of the senescent phenotype. The *est2* senescent cells were defined by their inability to proliferate compared to the wildtype control cells which are capable of

indefinite growth. Images of each streak were captured using a Canon Powershot G3 digital camera and saved as jpg formatted files.

Southern blot experiments

PCR amplification of nonradioactive DIG probe. DNA probes for Southern blot analysis were synthesized by PCR using an Applied Biosystems 2720 Thermal Cycler. Multiple reactions were performed using a prep of plasmid YTCA-1 that was diluted 1/100. One μ l of miniprep template DNA, 5 μ l primer M13 forward (5'-AGCGCGCAATTAACCCTCACTAAAG-3'), 5 μ l primer M13 reverse (5'-CAGGAAACAGCTATGACC-3'), 5 μ l 10x PCR buffer with MgCl₂, 5 μ l 10x PCR DIG labeling mix (2 mM dATP, 2 mM dCTP, 2 mM dGTP, 1.3 mM dTTP, 0.7 mM Digoxigenin-11-dUTP) and either 1 μ l Taq DNA polymerase were combined with sterile ddH₂O to bring each reaction to a final volume of 50 μ l. To serve as an unlabeled control, a reaction mix which included all of PCR additions above except for DIG labeling mix was run using 0.25 mM dNTPs instead. The reactions were then exposed to the following thermocycler conditions: 94 °C, 2 min and then 34 cycles: 94 °C, 30 sec, 49 °C, 30 sec, 72 °C, 1 min followed by a final extension period of 72 °C for 7 min. The PCR samples were run on a 3% agarose gel, stained with ethidium bromide and visualized on a Kodak Image Station 440 instrument.

DNA isolation and purification. Senescent cells that had been rescued via the telomerase expression system were harvested from colonies on gal-ura plates in 3 ml of YPGalactose broth and grown overnight in a 30 °C shaker. The DNA was purified using the MasterPure™ Purification Kit from Epicentre and DNA yield concentrations were quantified by fluorometry. Three μ g of DNA was digested overnight with restriction

enzyme XhoI in 1x KGB buffer at 37 °C. The digested DNA was then concentrated by ethanol precipitation and 1 µg of each sample was loaded onto a 1.2% agarose gel. Gel electrophoresis was carried out at 110 V in 1x TBE until the tracking dyes had migrated into the lower half of the gel. The gel was stained in ethidium bromide and destained in ddH₂O each for 10 min using gentle agitation. The gel was visualized under UV fluorescence to confirm that the DNA samples appeared properly digested and equal in concentration.

DNA denaturation and neutralization. After destaining and imaging, the gel was washed with denaturation buffer (1.5 M NaCl, 0.5 M NaOH) for 5 min at room temperature using an orbital shaker on low speed. Denaturation buffer was replaced and the gel was incubated for an additional 30 min. Next, the gel was washed in neutralization buffer (1.5 M NaCl, 0.5 M Tris, pH 7.5) for 5 min and then again with fresh solution for 30 min at room temperature. The DNA from the gel was transferred overnight onto a Hybond-N⁺ membrane (GE Healthcare) by employing a homemade capillary transfer apparatus which included blotting paper (VWR) and paper towels as wicks. The next day, DNA was fixed to the nylon membrane by UV cross-linking. The membrane was irradiated using a UV-Stratalinker 2400 (Stratagene) at 120,000 µJ energy for ~ 20 sec.

Probe hybridization. After UV cross-linking, the membrane was washed twice with ~ 30 ml of prehybridization/hybridization solution (DIG easy hyb granules from Roche) with shaking for 5 min at room temperature. The membrane was rotated in a glass roller bottle in 15 ml of prehybridization/hybridization solution for 60 min at 40 °C using a UVP HB-1000 Hybridizer hybridization oven. The digoxigenin (DIG)-labeled

DNA probe was denatured by placing it in 50% formamide solution and heated at 100 °C for 5 min and then was transferred to wet ice for 2 min. The prehybridization/hybridization solution was removed from the roller bottle using a pipet and replaced with 15 ml of fresh, pre-heated solution. Immediately following the ice bath, 100 µl of denatured probe was added to the roller bottle. The probe-containing solution was rotated over the membrane at 40 °C to hybridize overnight in the hybridization oven.

Detection by chemiluminescence. On the following day, the blot was removed from the overnight bottle and placed in a solution of 2x SSC/0.1% SDS (1:10 dilution of stock 20x SSC, 1:200 dilution of stock 20% SDS) and shaken using the orbital shaker at room temperature for 5 min twice. The blot was then washed twice for 15 min each in 0.5x SSC/0.1% SDS (1:40 dilution of stock 20x SSC, 1:200 dilution of stock 20% SDS) on a rocker tray at 55 °C. Next, the membrane was equilibrated in 100 ml washing buffer (10x washing buffer from Roche diluted to 1x) twice for 1 min each. The washing buffer was poured off and 150 ml of 1x blocking solution (10x blocking agent from Roche diluted to 1x) was added for 30 min with shaking. The blocking solution was then poured off and 40 ml of enzyme-linked antibody solution (6 µl antibody solution from Roche in 40 ml 1x blocking solution) was added for 30 min. Next, the antibody solution was poured off and the blot was washed twice with 100 ml of 1x washing buffer for 15 min each. This solution was poured off and the blot was incubated for 4 min with 40 ml detection buffer (10x detection buffer from Roche diluted to 1x). The blot was removed from the buffer and placed onto a pre-cut piece of clear plastic cling wrap. Using a P-1000, 1 ml of disodium 3-(4-methoxyspiro {1,2-dioxetane-3,2'-(5'-

chloro)tricyclo[3.3.1.1^{3,7}]decan}-4-yl) phenyl phosphate (CSPD) from Roche was aliquoted across the DNA-bound side of the membrane. The membrane was then immediately sealed using a second piece of cling wrap. The CSPD liquid was distributed across the membrane surface using fingertips and allowed to incubate at room temperature for 5 min. Next, all of the liquid was pressed out through the sides of the plastic sheets and the edges were sealed closed with tape. The blot was incubated again at 37 °C for 10 min. For imaging, the membrane was placed in a Spectroline Monotec X-ray cassette with 1 sheet of 8 x 10 in. MidSci Classic Autoradiography film. Intensifying screens were used and exposure times varied from 2 to 10 min before development.

CHAPTER III

RESULTS AND DISCUSSION

Telomeres are nucleoprotein protective structures at the ends of chromosomes whose functional integrity influences proliferative capacity, proper gene expression and genomic stability. In typical mammalian somatic cells, telomerase expression levels are nondetectable and telomere DNA shortening progresses with each round of mitosis. The telomere-associated protein complex is dependent upon telomere length and becomes disrupted upon reaching critically short levels. Without end-protection, chromosome termini are recognized as DNA double-strand breaks, subject to repair activities (35, 41, 42). This uncapping phenomenon, depicted schematically in Figure 3, occurs in telomerase-deficient yeast cells.

In yeasts and mammals, chromosome instability triggers cell cycle arrest through a DNA-damage checkpoint response (35, 42). During arrest with unprotected ends, the chromosome may be susceptible to recombination, telomere end-to-end fusions as well as exonucleolytic degradation (16, 42). In the event that cells are incapable of overcoming stress conditions, they may also induce apoptosis as an extreme response (42). An alternative model of senescence is that cells simply undergo permanent growth arrest without commitment to cell death.

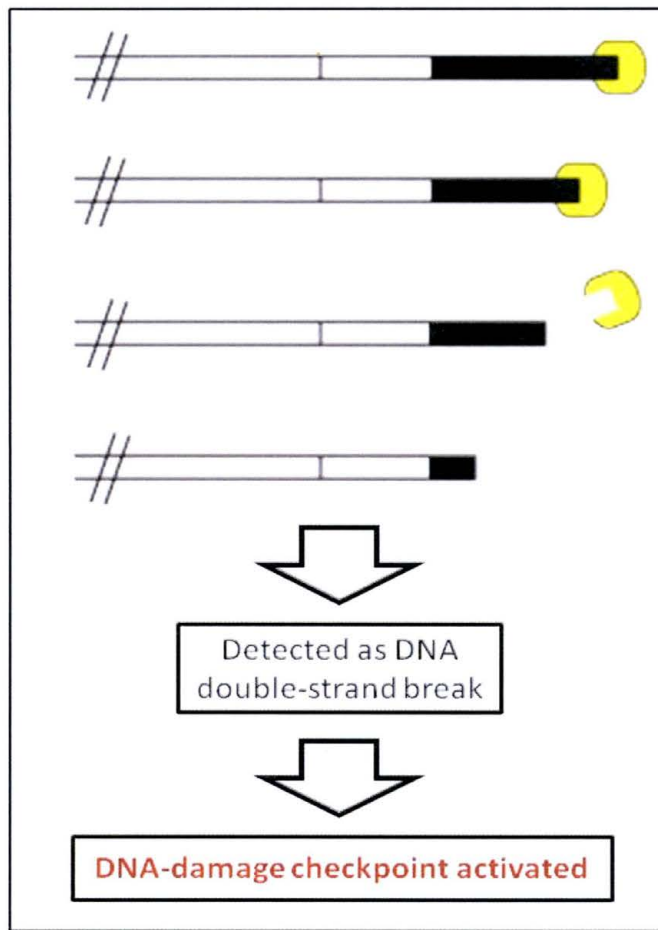


Figure 3. Schematic depiction of telomere shortening and protein uncapping processes. This presumably occurs *in vivo* and in cultured telomerase-deficient cells.

The precise cause of cell death during senescence is not clearly understood. This research project aimed to explore the aforementioned models of molecular changes that may develop during early and late senescence. A specialized haploid strain of the simple eukaryote, *Saccharomyces cerevisiae*, was utilized to model senescence.

Wildtype yeasts normally express telomerase and are unsusceptible to replicative senescence mediated by telomere dysfunction. A new yeast strain was developed in the

Lewis lab for simple regulation of telomerase activity *in vitro*. This was engineered by transforming telomerase-deficient cells with the plasmid pLKL82Y, which contains the catalytically active polymerase subunit of yeast telomerase (*EST2*) under the control of a modified galactose-inducible promoter, *GAL1-V10*. With the chromosomal copy of *EST2* deleted, this plasmid contains the only functional *EST2* gene in the cell. As shown in Figure 4, when the mutant cells are grown in the presence of the sugar galactose, the *GAL1-V10* promoter is strongly induced, driving the expression of *EST2*. Possessing telomerase activity, the telomeres are effectively maintained and the population possesses unlimited replicative potential. Conversely, when cells are propagated in media containing glucose, the *GAL1-V10* promoter has reduced basal expression and the *GAL1-V10p::EST2* fusion is turned off. This, in effect, eliminates telomerase activity, reduces proliferative capacity to 60-70 generations for most cells, and elicits cellular senescence (34).

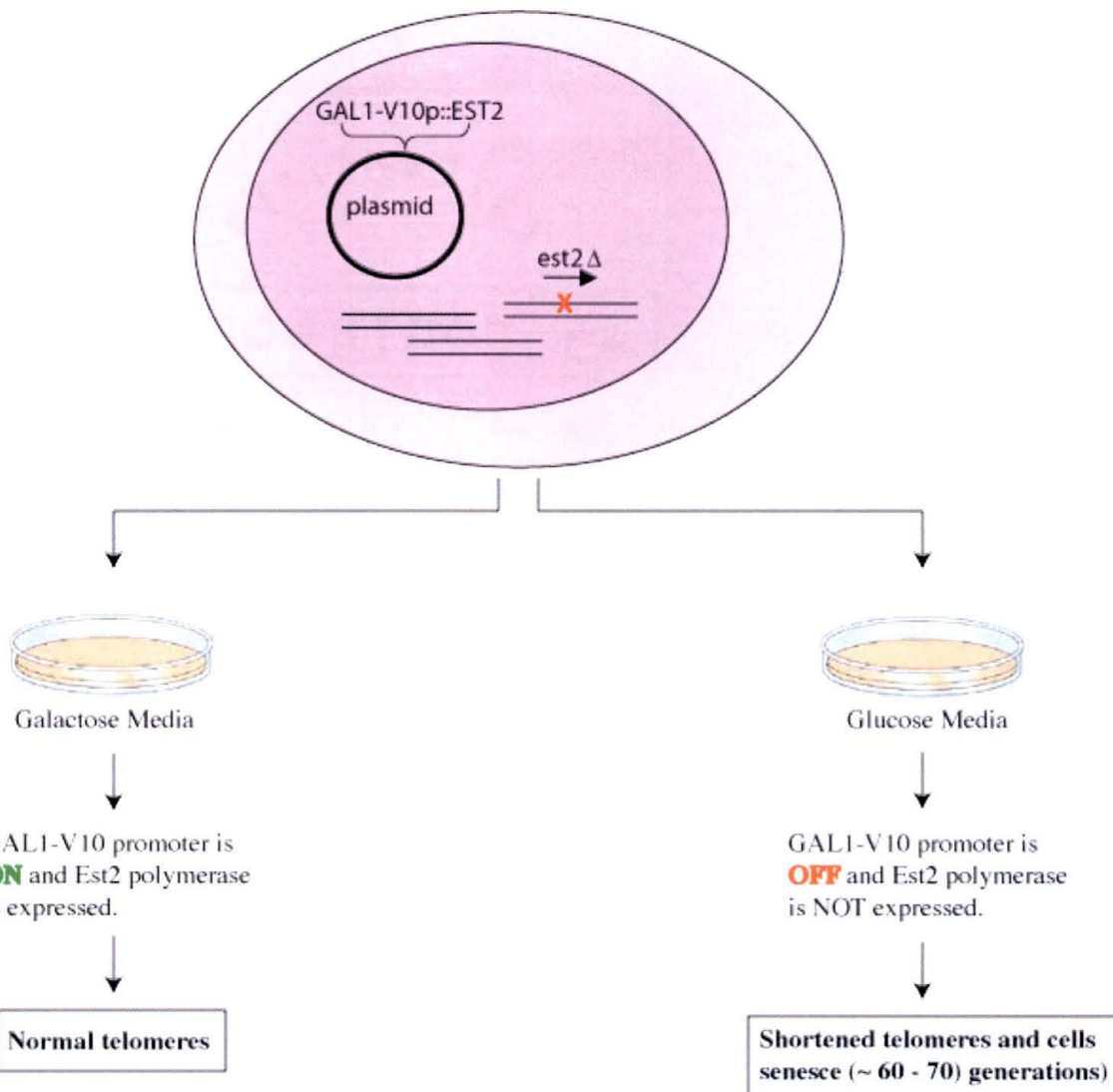


Figure 4. Illustration of the Est2 polymerase expression system indicating the activation (galactose media) or deactivation (glucose media) of telomerase.

To demonstrate senescence *in vitro*, telomerase-deficient yeast cells are streaked onto glucose-containing plates and grown for approximately 20 generations to form colonies (Figure 5). Cells from the first plate can be re-streaked onto fresh media, incubated, and will again re-form colonies after approximately 20 additional cell divisions. After similar re-streaking for a third streak, cells grow an additional 15-20

generations. By the fourth streak, cells of the senescing strain (YLKL803) consistently stop growing and cannot form normal colonies. At this point, cells have grown for about 60-70 generations and enter replicative senescence as a result of telomere dysfunction (38, 39).

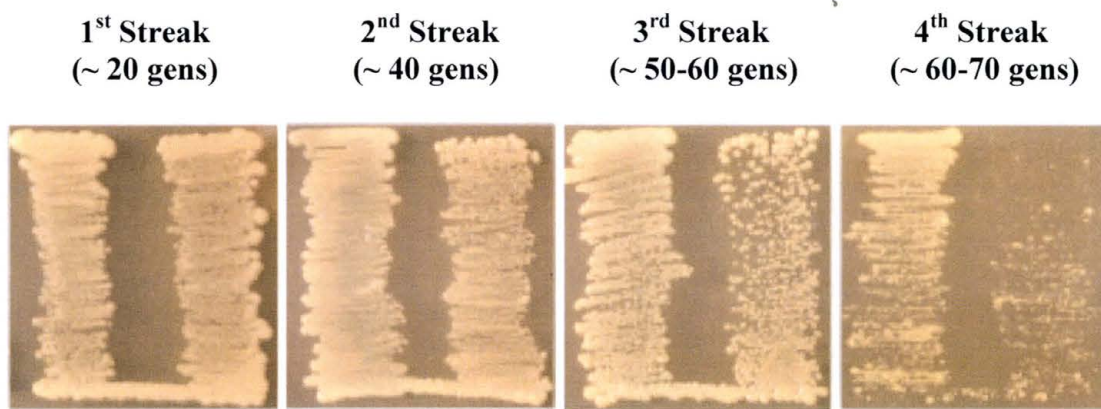


Figure 5. Column streaks of mutant *est2* cells grown on synthetic glucose plates. Senescence is exhibited on the fourth streak.

For the specific senescence assay shown in Figure 5, cells were streaked onto synthetic glucose minus uracil plates and incubated at 30 °C for ~ 72 hrs. For the first two streaks (~ 40 generations), cell growth was very robust, producing heavy colony density. The third streak had slightly fewer and more distinct colonies due to an overall increase in cell cycle delays. Senescence could be easily detected by the fourth streak, marked by a reduced ability to grow. These colonies displayed significant decreases in both size and overall numbers of colony forming units. This experiment demonstrated replicative exhaustion attained by telomerase-deficient cells, and established an estimation of the timing number of growth generations.

To assess DNA changes that accompany decreasing viability in aged cells, Southern blot analyses were performed to evaluate the rate and levels of telomere shortening. Prior to initiating these experiments, a telomere-specific probe labeled with digoxigenin (DIG) had to be accurately synthesized. DIG is an essential component of this nonradioactive Southern blot technique which utilizes an enzyme-linked immunoassay for detection. The probe was prepared by PCR amplification of a purified template DNA complementary to *S. cerevisiae* telomere DNA. Through PCR, the thermostable Taq DNA polymerase incorporated DIG-dUTPs as it amplified a specific region of the template DNA (Figure 6).

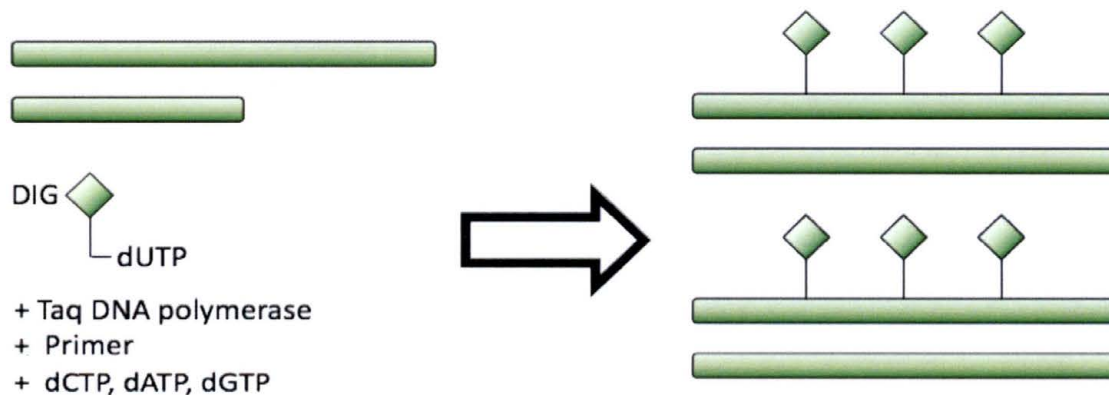


Figure 6. Illustration of PCR labeling digoxigenin (DIG) labeled dUTP to generate a DNA probe for Southern blot experiments.

The ends of every chromosome contain a highly conserved, TG-rich, tandemly repeated DNA motif that is targeted by the Southern blot probe for hybridization. Using the DIG system, probe-target hybridization is detected with an alkaline phosphatase-

conjugated antibody that produces a chemiluminescence reaction in the presence of CSPD (Figure 7). The antibody is specific for DIG and recognizes DIG molecules on the labeled hybrid.

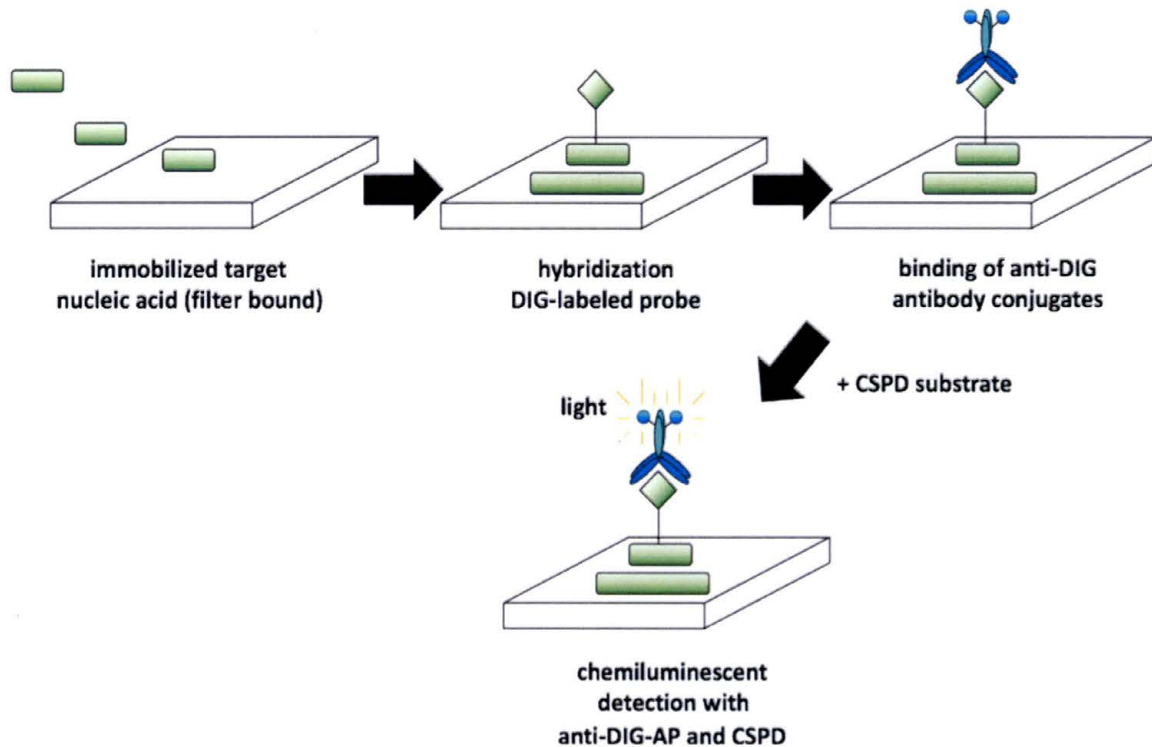


Figure 7. Illustration of the immunochemical detection method for Southern blot experiments. DIG-labeled DNA probes are used to detect DNA targets, followed by an enzyme-linked antibody reaction to produce chemiluminescence.

Prior to use, the telomere probe PCR product yield was checked using agarose gel electrophoresis. Both DIG-labeled and unlabeled dNTP reactions were performed. The unlabeled product was synthesized using the same reaction mixture under identical conditions as the DIG-labeled dUTP-containing reactions, except that the four standard

dNTPs were used. Once electrophoresis was completed, the gel was stained with ethidium bromide and digitally photographed (Figure 8). Bands from the DIG-labeled samples migrated at approximately 250 bp in size as expected and produced satisfactory yields.

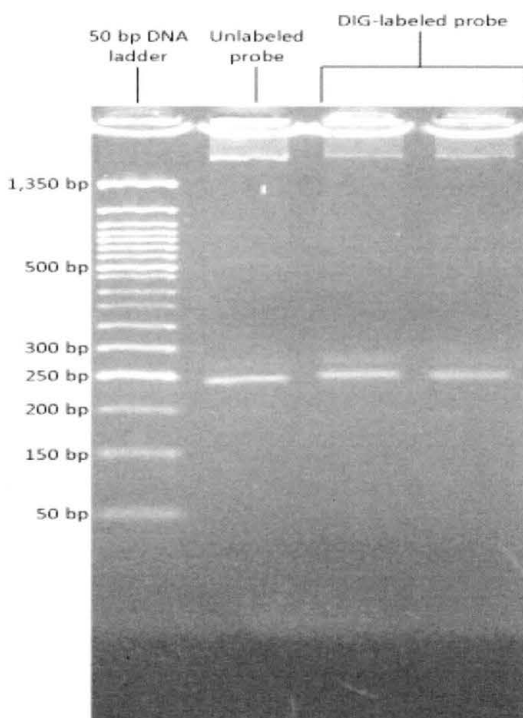


Figure 8. Confirmation of the synthesis of a DIG-labeled probe on a 3% agarose gel.

Prior to initiating a test Southern blot for this project, *S. cerevisiae* chromosomal DNA was digested using the restriction endonuclease XhoI. This enzyme was specifically chosen because of the location of an XhoI restriction site within the subtelomere region on a majority of the yeast chromosomes. The digested DNA samples were separated by agarose gel electrophoresis followed by ethidium bromide staining.

Upon UV exposure, the samples appeared as an intense upper band of large DNA with an underlying short smear representing XhoI-digested chromosome fragments (Figure 9). The sensitivity of ethidium bromide staining is poor and is largely inadequate for detecting DNA in low concentration. Also, when used alone, it is impractical for targeting specific DNAs of interest. Southern blotting, in contrast, is a highly advantageous technique displaying exceptional sensitivity for target detection. After staining, the DNA was transferred from the agarose gel directly onto a nylon membrane followed by target probing. After incubation with DIG antibody and enzyme followed by addition of the substrate CSPD, the blot target probing was visualized using x-ray film (Figures 9 and 10).

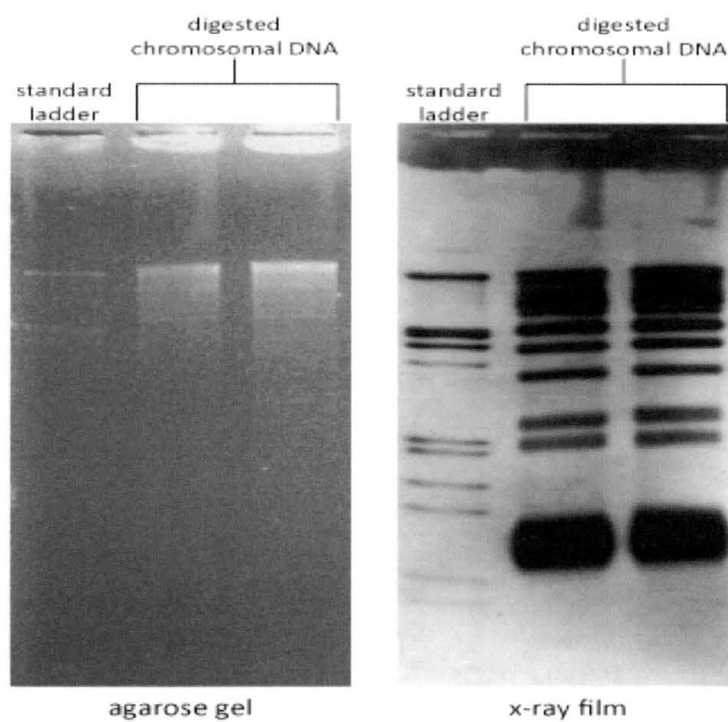


Figure 9. Digested yeast chromosomal DNA visualized on an agarose gel (right) and subsequent assay by Southern blotting, visualized on x-ray film (left).

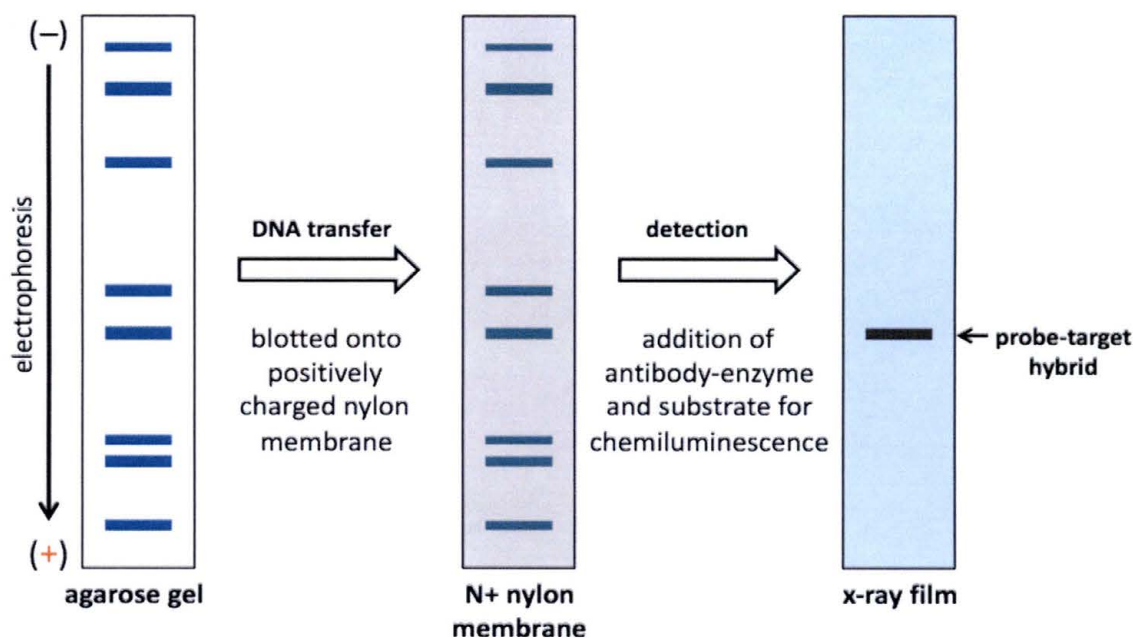


Figure 10. The Southern blot technique. Southern blotting combines the transfer of electrophoresis-separated, digested chromosomal DNA fragments onto a nylon membrane with subsequent probe-target hybridization and detection.

The aim of this project was to employ Southern blot analysis to monitor telomere lengths and evaluate post-senescent molecular changes. Before performing these primary analyses, the telomere fragment profile of *S. cerevisiae* DNA was studied in order to improve interpretation of Southern blot banding patterns. DNA from wildtype (*EST2*) cells (BY4742) was purified and then digested with *Xba*I. Southern blot analysis using a standard 1.2 % agarose gel revealed 6 discreet lower bands and an upper aggregate of unresolved high molecular weight bands (Figure 11).

A separate Southern blot was performed to resolve the upper bands by extending the electrophoresis duration by about three times and using 1% agarose concentration. By increasing overall fragment migration, the ‘extended-run’ Southern blot revealed 9 upper telomere bands indicating a total of 15 (Figure 12). Fragments under 6,000 bp

migrated completely off the gel, accounting for the absence of the lower 6 bands. Greater band separation also allowed for improved distance determination and hence, increased accuracy in quantitating fragment sizes.

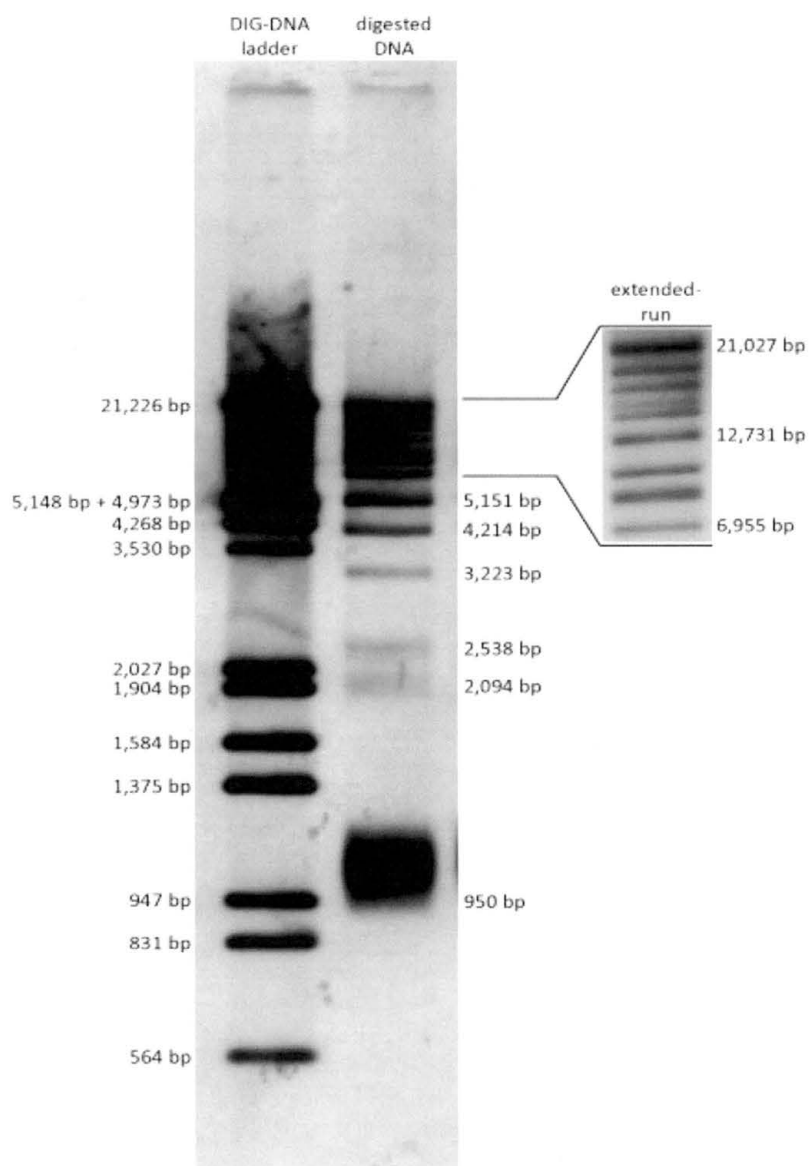


Figure 11. Southern blot detection of *S. cerevisiae* chromosome ends. XhoI digestion produced 15 bands, ranging from 21,027 to 950 bp.

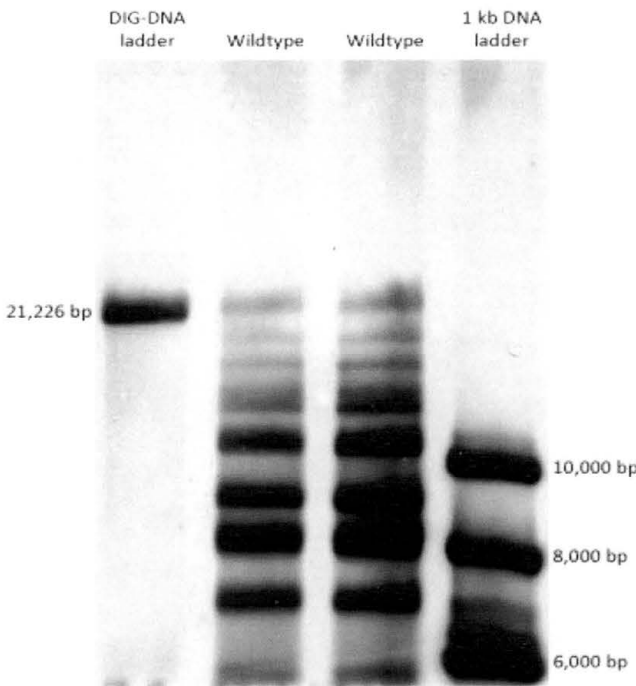


Figure 12. Southern blot performed to resolve upper (high molecular weight) bands in the top portion of the gels. Increased migration displaced the lower bands from the gel.

Sizes of the DNA fragments (bp) were quantitated based on a standard curve.

This was accomplished by first measuring migration distances (mm) of each individual band within the molecular weight ladders. Each band featured in the standards has a known molecular size (bp). A chart was constructed from this data, plotting migration distances versus the log of the base pairs for each band (Figure 13). From these data, a best fit line was generated and the standard curve linear expression was obtained. The measured distance of each of the 15 telomere-containing bands were substituted into the linear formula (y variable) and the fragment sizes (x variable) were algebraically calculated. The calculated sizes for several of the telomere DNA fragments are displayed in Figure 11.

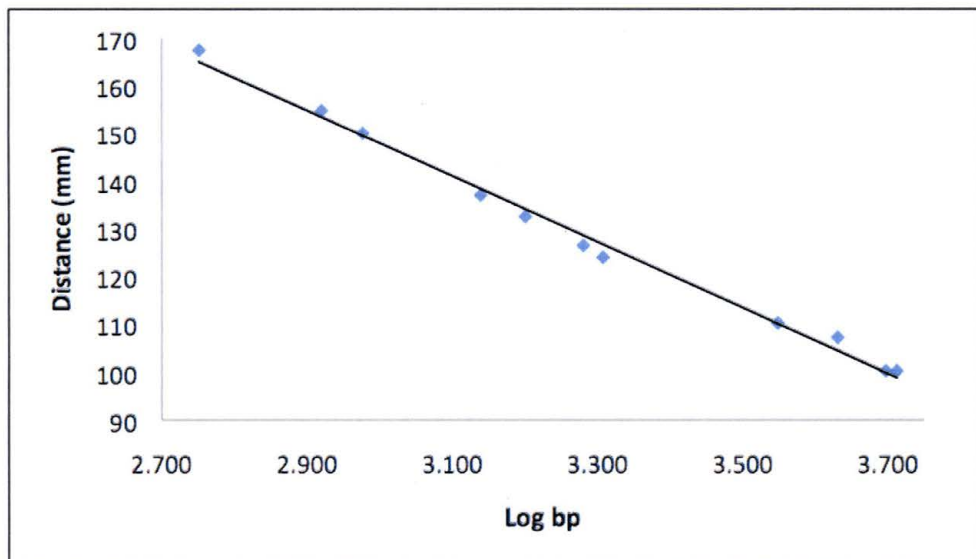


Figure 13. Standard curve for telomere length quantitation. Linear regression analysis of telomere fragment sizes (bp) is based on migration distance of the molecular weight standards. The trend line is displayed and is represented by the equation: $y = -68.84x + 354.49$.

The migration distance of DNA bands in the Southern blot assay revealed significant differences in chromosome end fragment sizes. These size differences are a result of the variability of the XhoI restriction site locations proximal to the telomere ends (Figure 14). The greater the distance from the restriction site to the end of the chromosome, the larger the resulting fragment will be. There are a total of 16 chromosomes in *S. cerevisiae* cells, which means that the chemiluminescent signals produced in these Southern blots should be derived from 32 different chromosome ends.

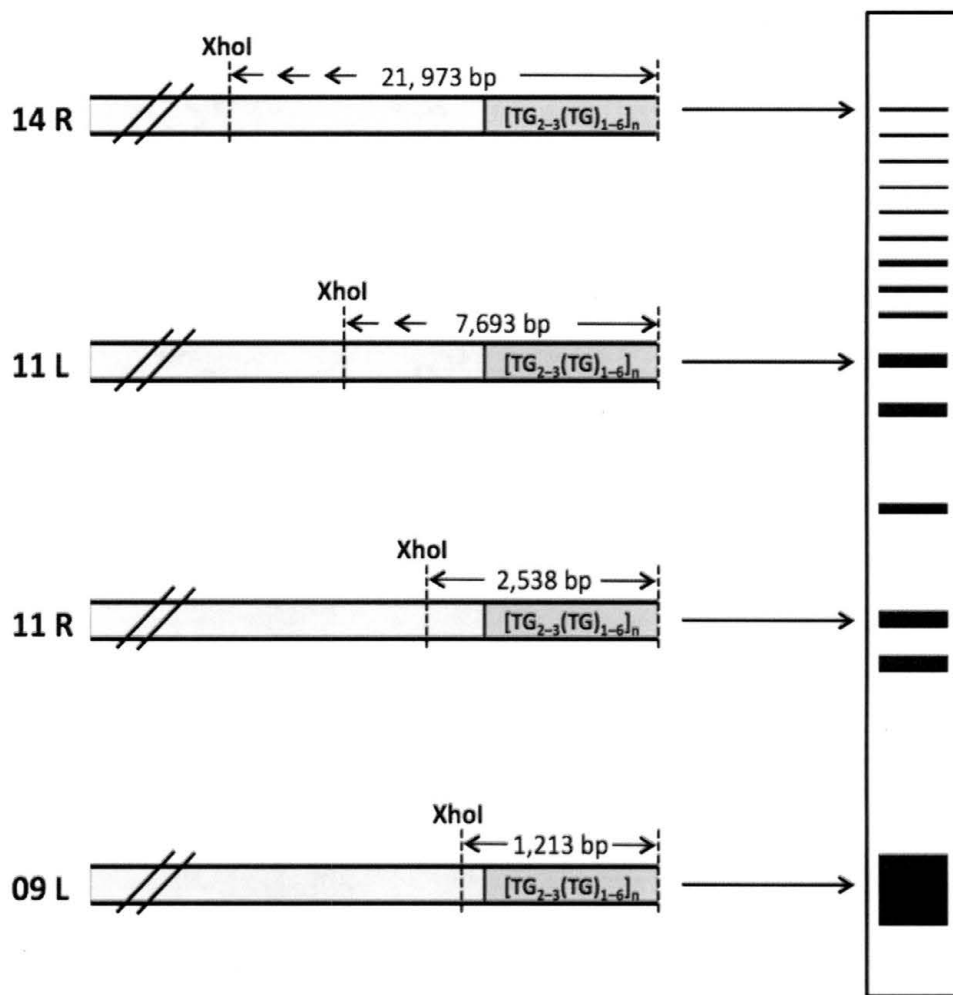


Figure 14. Example illustrating the differences in band size, as seen in Southern blots. The location of the terminal *Xhol* restriction site typically varies on each chromosome (L, left arm; R, right arm).

In addition to identifying both the number and sizes of all bands seen in Southern blots, an additional study was performed to compare these results to an expected band pattern, based on published subtelomere and telomere DNA sequences for the *S. cerevisiae* genome. This information was obtained from a database accessed through the University of Nottingham Institute of Genetics website. Sequenced DNA of the Crick strand was arranged by chromosome number (1-16) and chromosome arm (left or right)

(<http://www.nottingham.ac.uk/genetics/people/louis/>). Each set was analyzed computationally to identify all XhoI sites by copying the entire DNA sequence into NEBcutter, an online sequence analysis program (<http://tools.neb.com/NEBcutter2/>).

None of the telomere sequences was complete, likely because of limitations of cloning and sequencing methods. The telomeres of *S. cerevisiae* are typically reported to be in the vicinity of 350 bp in length. Since these regions consist solely of TG-rich DNA repeats, the precise telomere starting points were discerned from the subtelomeric region by position of the terminal adenine or cytosine. This base is located immediately upstream to where the Ts and Gs of the telomere sequence begin. These exact locations were used to determine the precise distance (bp) from the terminal XhoI site to the telomere start sites for each chromosome. To account for incomplete end-sequencing, 350 was added to the each calculated distance. This reflects the actual sizes (bp) of the telomere fragments generated by XhoI digestion that undergo hybridization and detection in the Southern blots (Figure 15).

Identification of the positions of XhoI sites near each chromosome end allowed prediction, for the first time, of the expected sizes of all 32 telomere fragments. These deduced sizes were then used to simulate a Southern blot. This theoretical blot is shown in the left side of Figure 15. A total of 14 bands were predicted. Two bands are predicted to be “doublets”, having two fragments of approximately the same size, and one predicted band has three different fragments (5151, 5160 and 5177 bp). One band near the bottom of the gel is very broad, ranging in size from 1,028 to 1,222 bp and is predicted to represent 15 different ends. The projected Southern blot was compared to the actual Southern blot band pattern observed using yeast strain BY4742 (Figure 15),

which revealed strong similarity. There were two bands (17,052 bp and 14,660 bp) that were detected experimentally, but were not predicted based on the published sequences. As for the projected Southern blot, there is one small predicted band not seen in the actual blots (496 bp).

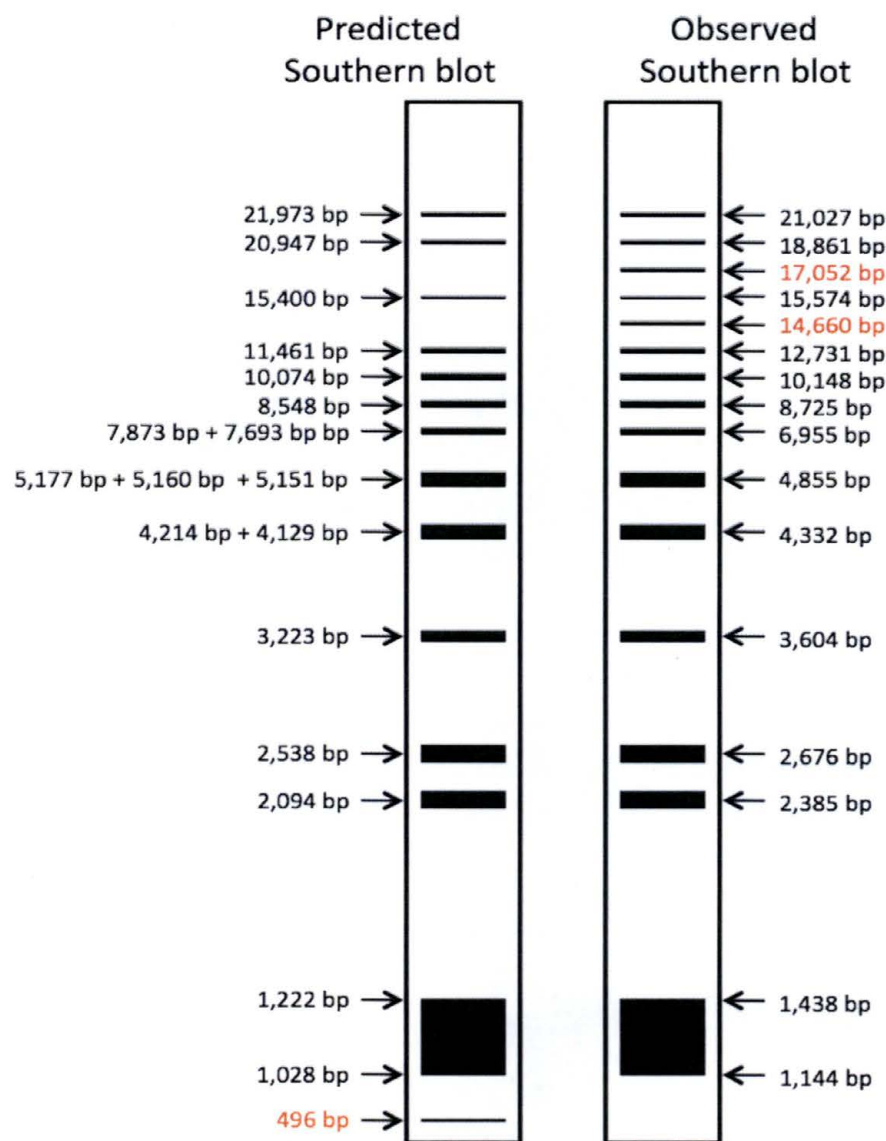


Figure 15. Telomere bands detected experimentally (right) compared to the projected band pattern of XhoI digested, BY4742 (wildtype) DNA (left).

As shown in Figure 15 and 16, the calculated fragment sizes were compared to the published sequences to match chromosome ends with corresponding bands. Chromosome ends were assigned to bands based on percent agreement between calculated and predicted fragment sizes. Twenty-nine out of 32 chromosome arms were matched. Of the 15 bands detected in the blots, at least one single chromosome could be confidently assigned to 10 of these with a percent difference of 10% or less. As stated earlier, two bands are present in the observed blots that are not supported by the published sequences. The overall average percent difference is 7.1%.

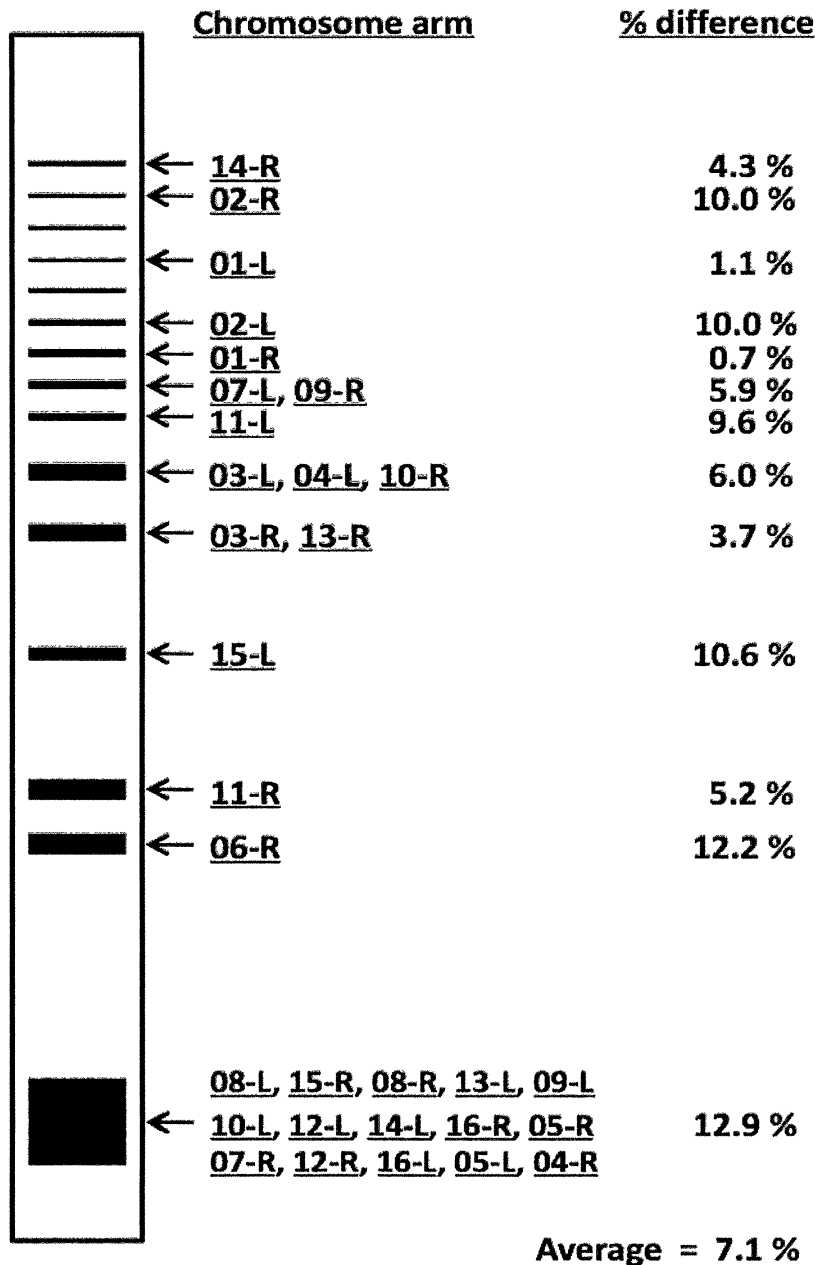


Figure 16. Assignment of chromosome ends to Southern blot bands. Results are based on a published sequence of *S. cerevisiae* telomeres and subtelomeres (L, left arm; R, right arm). The % difference indicates agreement between predicted and observed telomere sizes.

Saccharomyces cerevisiae is a genetically tractable model system for studying genetics and molecular biology of eukaryotes. The ability to isolate genomic DNA from this organism is essential for a multitude of molecular techniques including Southern blots. Despite the commonplace application, there exists little scientific literature addressing yeast DNA purification. Traditionally, yeast cell walls have been lysed using an enzyme preparation of either beta-1,3-gluconase (lyticase) or zymolyase (40). This enzyme-based approach can be tedious and performance is variable. As an alternative, physical disruption by mixing cells with glass beads has been employed, but this approach shears the DNA into small fragments (38, 40).

Chemical-based DNA purification methods are relatively simple to use and are favored over alternative methods for cell wall disruption. Due to the scarcity of published protocols, many laboratories are dependent on expensive, chemical-based commercial purification kits. This phase of the current research project aimed to establish a new chemical-based protocol for purifying yeast chromosomal DNA to be used in Southern blots. A series of experiments were carried out to modify reagents and determine conditions for maximal DNA recovery.

The initial selection of reagents for DNA purification was modeled, in part, after those described in a published article for yeast genomic DNA purification. In that study (40), cell suspensions were treated with 3% sodium dodecyl sulfate (SDS), a detergent used to disrupt cell membranes and cell walls, in the presence of 0.2 M NaOH. The authors also reported that heating cell solutions suspended in SDS plus NaOH during purification did not substantially improve cell lysis and DNA yields. Using this resource as a guide, the first of several purification experiments commenced.

In the initial experiment, cell disruption and extraction were carried out in a 3% SDS solution. Ten mM EDTA was included in all purifications to inhibit DNase activity by chelating Mg²⁺ ions. Four different sets of experimental conditions were tested with 3 individual samples purified per set.

The basic protocol used for this and most other experiments involved growing yeast cells (strain BY4742) overnight in YPDA liquid media and purifying DNA from 3 ml cell solutions. Cells were pelleted by centrifugation, resuspended in 300 µl of cell lysis (SDS) solution containing EDTA and heated or not heated at 65 °C for 15 min. Either sodium acetate (NaOAc) or potassium acetate (KOAc) (150 µl) was added to precipitate proteins and cell debris, followed by centrifugation for 15 min. The supernatant containing nucleic acids released from the cells was transferred to a new microfuge tube, precipitated with 500 µl isopropanol, washed with 70% ethanol, dried under vacuum and the DNA was resuspended in 50 µl TE. DNA concentrations were quantitated by fluorometry and protocol performances were evaluated based on comparison of relative yields. The conditions tested for the first experiment can be summarized as follows: (1) 3% SDS + 0.2 M NaOH without heating (as in the previously published protocol), (2) 3% SDS + 0.2 M NaOH with 65 °C heating step, (3) 3% SDS only without heating, and (4) 3% SDS only with 65 °C heating step.

Results revealed that heating had no substantial effect on the efficiency of the method for samples purified using SDS plus NaOH and yields were 98 and 119 µg/ml (Figure 17). Unheated SDS minus NaOH solution produced similar results, with a DNA yield of 112 µg/ml. In contrast, SDS alone with heating produced an average DNA concentration of 301 µg/ml. This equates to an approximate three-fold increase in yield.

Based on this significant increase, the cell lysis solution for all subsequent purification experiments thereafter excluded NaOH and included a 65 °C heat treatment.

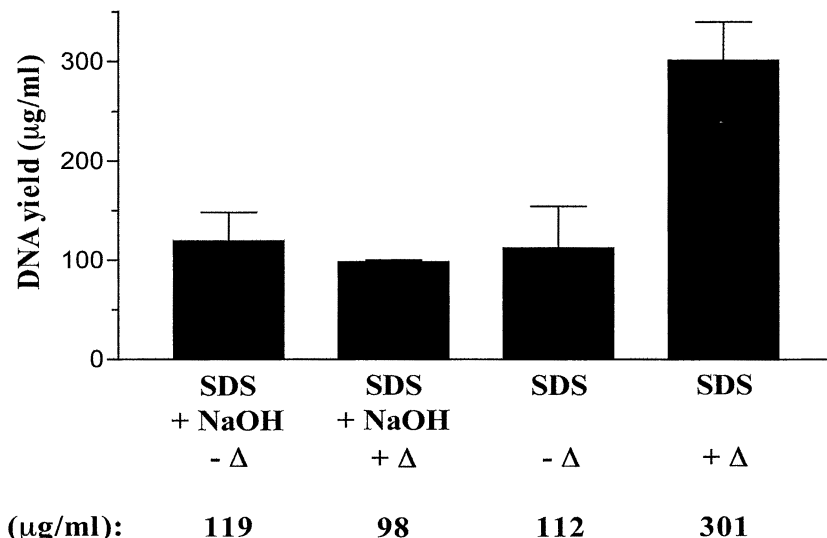


Figure 17. Average DNA concentrations of yeast chromosomal DNA purified using 3% SDS cell lysis solutions, with or without 0.2 M NaOH, and a 65 °C incubation period. Error bars indicate standard deviations ($n = 3$).

The initial purification experiment established two important extraction conditions for DNA purification and served as a basis for subsequent experiments. The efficacy of the protein precipitation reagent, a second critical component, was next evaluated in a head-to-head comparison. The protocol was repeated as before except that 3 M potassium acetate (KOAc) was substituted in place of NaOAc for precipitation of proteins. Product yields quantitated by fluorometry revealed a 78% increase in average DNA concentration for purifications using KOAc (Figure 18). The increased product yield was reproducible in additional experiments and KOAc was used in all ensuing tests.

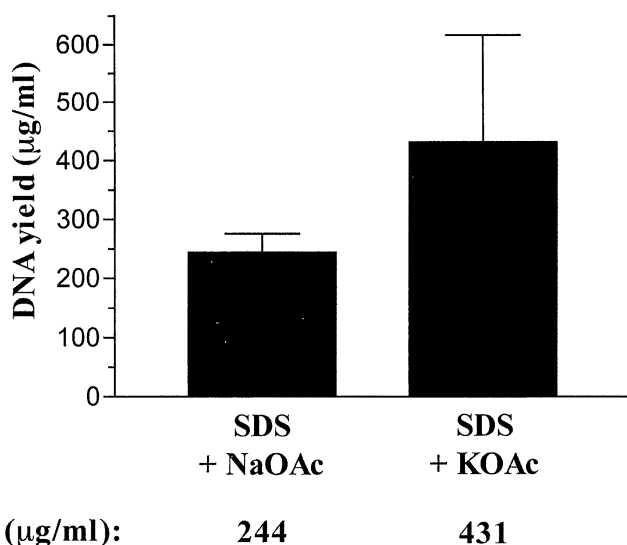


Figure 18. Average DNA concentrations after different protein precipitation reagents were used for DNA purification. Potassium acetate solution produced a 78% increase in DNA yield over NaOAc.

The sizes of the purified DNAs were checked using agarose gel electrophoresis. Equal volumes of resuspended DNA solutions were electrophoresed on 0.6% agarose gels, stained, and digitally photographed. The sample purified using KOAc solution is shown as a DNA band of greater fluorescence intensity relative to that utilizing NaOAc (Figure 19). Since fluorescent output is proportional to DNA concentration, this observation supports fluorometry measurements. In effect, a significantly higher DNA yield is confirmed. Also, co-migration of the bands reveal that both samples are equal in size and consist of high quality (high molecular weight) chromosomal DNA fragments sheared to an average size of approximately 50,000 bp.

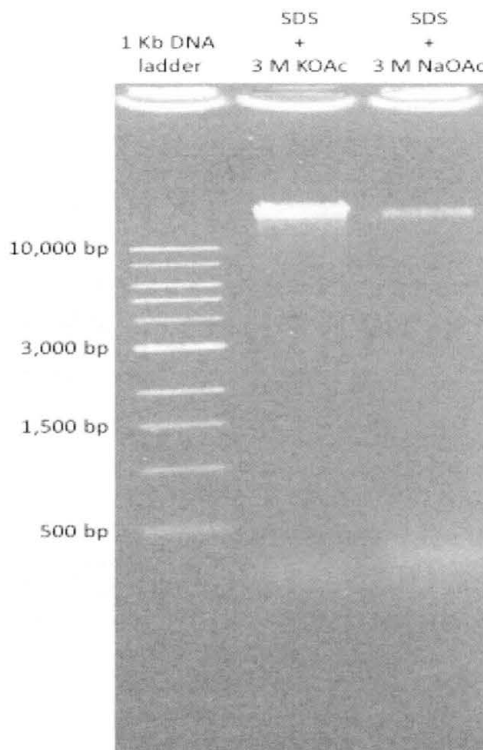


Figure 19. Agarose gel electrophoresis of purified DNA samples each using a different alkali precipitation reagent.

An experiment was proposed to evaluate if increasing SDS detergent would enhance cell lysis and therefore increase DNA yield. Solutions of 3, 6, 9, and 12% SDS concentrations were prepared and DNAs purified using the same basic protocol (SDS + 65 °C heating, followed by protein precipitation with KOAc). The products were quantitated using fluorometry and then evaluated based on average yields. Results indicate that increasing SDS does increase DNA yield but only marginally (Figure 20). The range of yields was from 431 µg/ml to 498 µg/ml. The difference from lowest-to-highest (67 µg/ml) was smaller than the standard deviations, and therefore the differences are not statistically significant. The average yield using 6% SDS was slightly greater

than that of previously used 3% SDS, and practically indistinguishable from 9%. Despite producing slight increases in DNA yield, a cloudy supernatant DNA solution containing insoluble particulates was observed in both 9 and 12 % SDS supernatants after addition of KOAc and centrifugation. As a result, 3-6% SDS solutions were deemed optimal and 6% SDS was chosen for use in subsequent experiments.

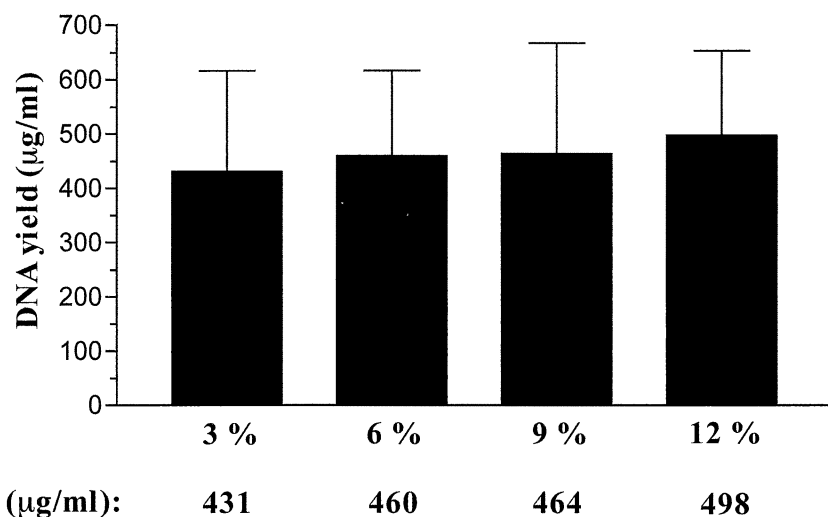


Figure 20. Average concentrations of yeast chromosomal DNA purified using different concentrations of SDS.

The effects of pH buffering on the efficiency of extraction were addressed next. The article referenced for this project (40) described resuspending yeast cells in buffer containing 10 mM Tris prior to cell disruption. To test whether the presence of a buffer positively influences purification, new reagents were prepared by adding various concentrations of Tris buffer (pH 8) to the SDS lysis solution. The 6% SDS solution was compared to 6% SDS combined with 10, 30, or 50 mM Tris. Use of 10 and 50 mM Tris produced average DNA concentrations less than that of 6% SDS without Tris (Figure 21).

Thirty mM Tris in SDS solution was the top yielding reagent, resulting in the highest yield (260 µg/ml) for the experiment. This result was also reproduced in subsequent experiments (data not shown). The pH of the original 3% SDS lysis solution was 7.7 and this changed to 8.5 after addition of 30 mM Tris (pH 8.0). It is not clearly understood why the presence of the buffer enhanced DNA yields, but this addition was adopted as the new standard.

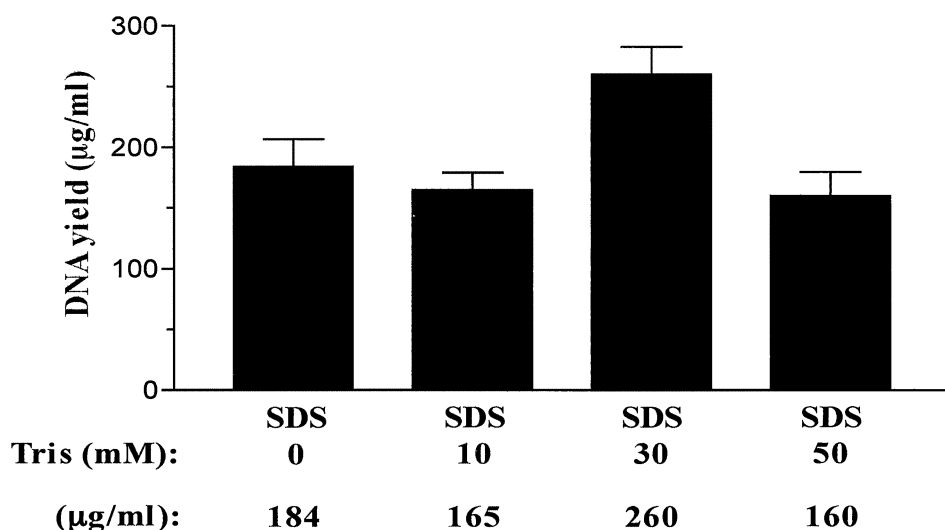


Figure 21. Average DNA yields quantified from purifications performed using 6% SDS solutions with and without increasing concentrations of Tris buffer.

Based on previous experimental outcomes involving lysis without Tris, 6% SDS was the optimal reagent for extraction purposes. A second evaluation was performed to investigate the effects of variable detergent concentrations using the new SDS plus Tris cell lysis solution. Cell lysis solutions were prepared by adjusting SDS concentrations to 3, 6, 9 and 12%, including 30 mM Tris buffer for each. DNA quantitation after

purification revealed a consistent trend of product yield increase with increasing SDS (Figure 22). Nine and 12% SDS solutions were again deemed unfavorable based on formation of a cloudy supernatant after KOAc addition and subsequent centrifugation.

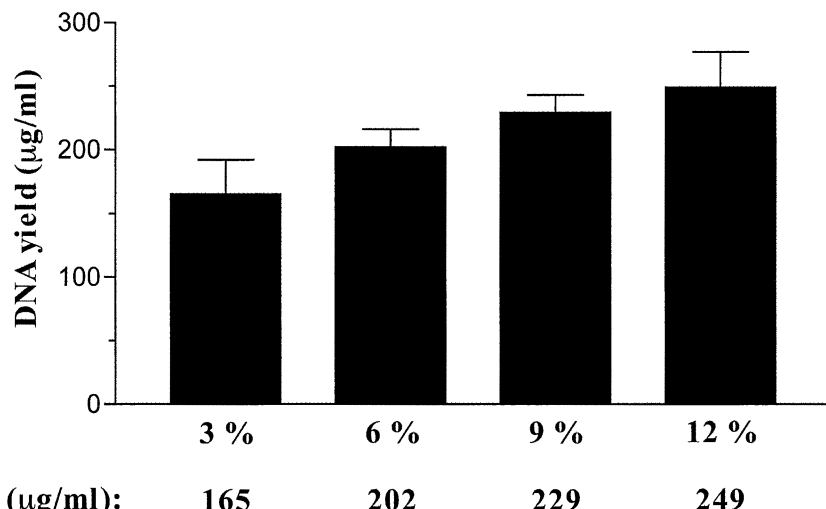


Figure 22. Average DNA concentrations of samples purified using cell lysis reagents with 30 mM Tris buffer and variable SDS concentrations.

Equal sample volumes from each set were loaded onto a 0.6% agarose gel and visualized by UV fluorescence (Figure 23). Relative band intensities appear approximately equal, indicating that each reagent can be successfully employed to purify yeast chromosomal DNA regardless of SDS concentrations tested. Fluorescence seen at the bottom of each lane corresponds to small molecular weight RNAs that are weakly stained by ethidium bromide.

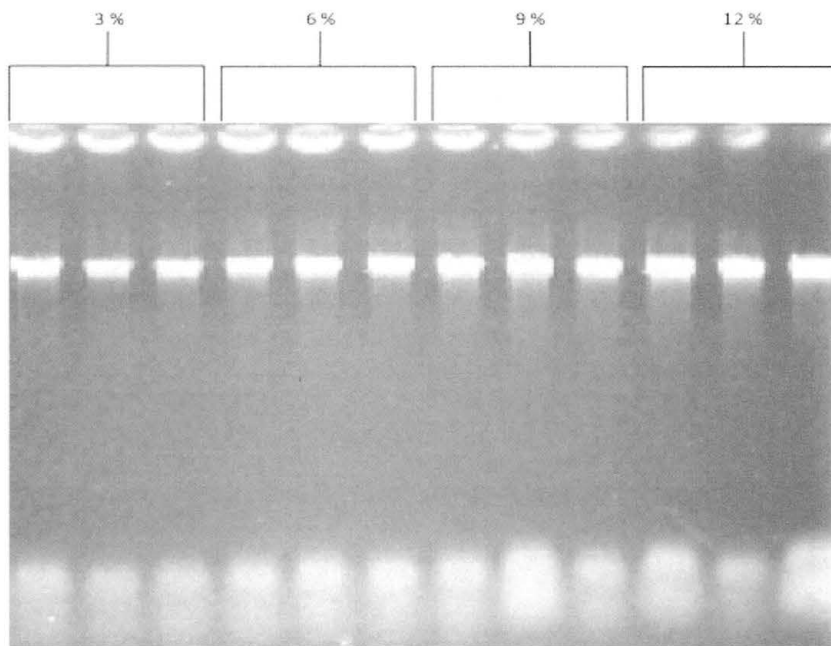


Figure 23. A 0.6% agarose gel showing fluorescent bands of yeast chromosomal DNA purified using variable SDS concentrations with Tris.

To test performance of the different SDS methods, 6% SDS alone and 6% SDS with 30 mM Tris were compared to a commercial yeast DNA purification kit (Epicentre). This kit, called the Masterpure Yeast DNA Purification kit, involves addition of cell lysis and protein precipitation reagents to yeast cells, similar to the new SDS protocols, but the composition of the kit solutions is proprietary and therefore unknown. Each set of samples followed an identical purification protocol, differing only in the chemical reagents used. Surprisingly, the SDS methods outperformed the commercial reagents (Figure 24). In comparison to samples purified using the Epicentre kit, SDS alone resulted in a 24% increase in average product yield while SDS supplemented with Tris produced a substantial 60% increase.

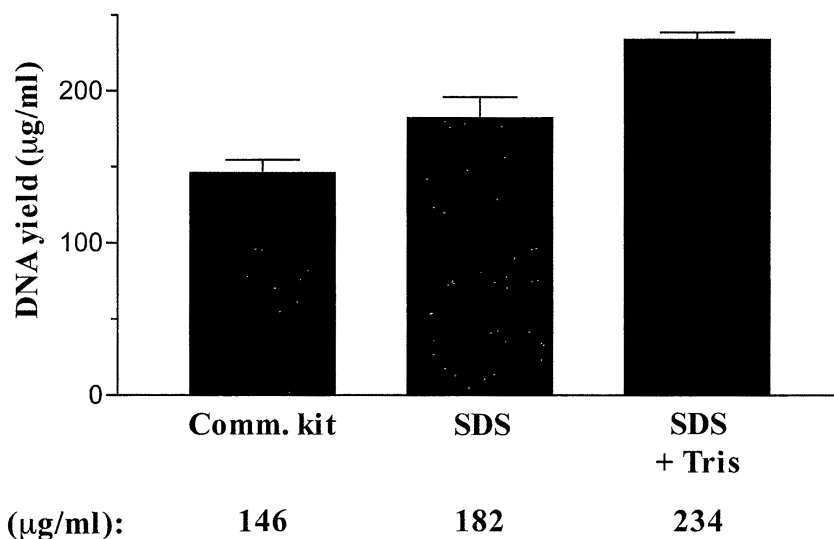


Figure 24. Comparison of average DNA concentrations of purified product using the SDS method versus a commercial kit for yeast chromosomal DNA purification.

DNA samples prepared using the SDS-methods were checked against DNA purified using the Epicentre kit. Equal volumes of resuspended DNA samples were run on a 0.6% agarose gel and DNA yields from the 6% SDS cell lysis solution and 6% SDS with 30 mM Tris buffer were compared to those of the commercial kit (Figure 25). The homogeneity in the band pattern indicates that the genomic DNAs are nearly equal in size. The sets purified using SDS with Tris appear to emit greater fluorescence, confirmation that the SDS method exceeds the performance of the commercial kit for yeast chromosomal DNA purification.

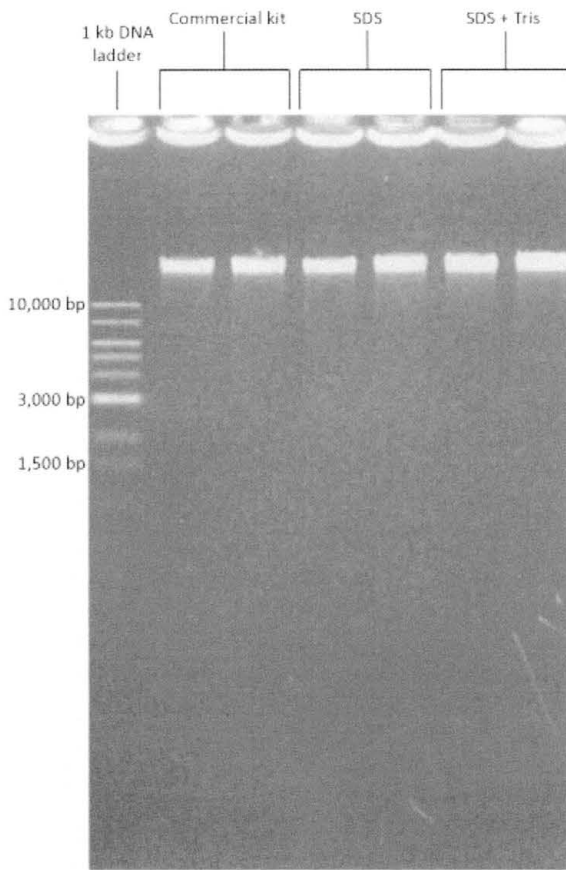


Figure 25. Agarose gel electrophoresis to compare relative DNA concentrations based on differential fluorescent band intensity. The SDS methods of purification is compared to the product yield of a commercially available kit from Epicentre.

In this project as well as many other lines of research, yeast chromosomal DNA is routinely digested using restriction endonucleases. Since this procedure is used in conjunction with DNA purification, it is pivotal that purified DNA is an effective substrate for restriction enzymes. Without this capability, the practicality of a DNA purification protocol would be negated. To address this concern, an experiment was carried out to assess the digestibility of DNA purified using the SDS method. Equal amounts of purified DNA underwent EcoRI digestion followed by electrophoretic

separation on a 0.6% agarose gel (Figure 26). Results were compared to DNA purified using the Epicentre kit. For each sample, fluorescence detection revealed a long smear of short DNA fragments. This result was consistent with complete digestion of chromosomal DNA.

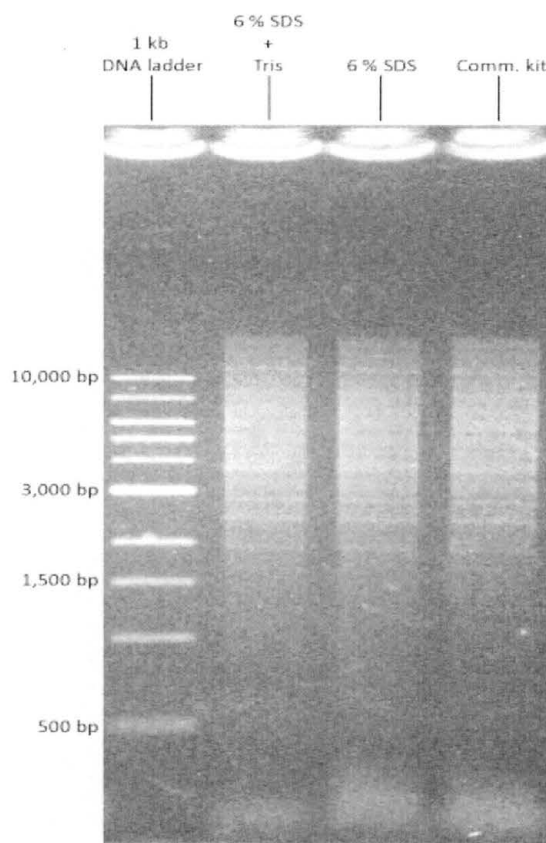


Figure 26. A 0.6% agarose gel separating fragments of yeast chromosomal DNA digested with EcoRI following purification using three different sets of reagents.

The next phase of the project involved use of Southern blotting to measure the average sizes of telomere fragments during the process of senescence. In order to

evaluate the rates of telomere attrition in aging yeasts, cells of the telomerase-deficient YLKL803 strain were grown to reach senescence. Over the course of 3 plate streaks, cells proliferated approximately 55-60 generations and entered senescence. Cells from the 1st, 2nd, 3rd streaks were harvested, DNA was purified, and chromosomes were digested with XhoI for Southern blot analysis. As shown in Figure 27, the telomere bands became progressively shorter during each streak.

Telomere fragment lengths were quantitated through distance measurements of the lowest DNA band. This lower band represents approximately 15 chromosome ends for *S. cerevisiae* and is the most sensitive to changes in molecular weight because of its small size. The average length of the lower fragment in DNA of wildtype cells (non-senescing) was maintained at 1119 bp (Figure 27 and Table 1). DNA from the first streak had a calculated telomere length of 1008 bp (shown in Table 1 under the column heading Fig. 27). The size for DNA from the second streak was 956 bp and 907 bp for the third. At the point of the second and third streaks, there was on average approximately 50 bp of telomere DNA lost over each of the 20 generations of growth. After streak 3 (55-60 generations), the cells become senescent and incapable of forming normal colonies. These results taken from Figure 27, as well as average lengths based on data obtained from 3 separate Southern blot experiments are summarized in Table 1. The telomere fragment length was reduced from 1100 ± 13 to 927 ± 37 bp when 3 experiments were averaged.

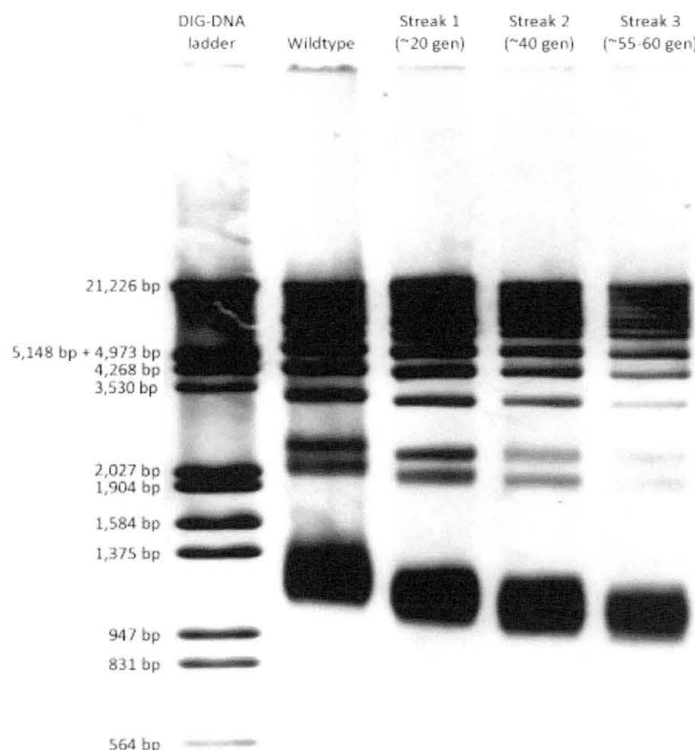


Figure 27. Southern blot analysis of telomere fragment lengths after XbaI digestion of YLKL803 (*est2*) chromosomal DNA. This assay shows progressive telomere shortening during replicative senescence.

Table 1. Calculated fragment sizes (bp) of the lower band observed in Southern blots used to evaluate telomere length after multiple generations in telomerase-deficient cells. Gens, number of generations of growth before DNA was harvested.

Sample	Growth (gen)	Fig. 27 (bp)	Average (bp)
1 st Streak (<i>est2</i>)	~ 20	1008	1033 ± 22 ^a
2 nd Streak (<i>est2</i>)	~ 40	956	974 ± 23 ^a
3 rd Streak (<i>est2</i>)	~ 55-60	907	927 ± 37 ^a
Wildtype (<i>EST2</i>)	---	1119	1100 ± 13 ^a

^astandard deviation

To address critical questions concerning the reversibility of cellular senescence, a previous graduate student in the Lewis lab, Sandra Bacerra, demonstrated that most senescent (non-growing) cells could be rescued if telomerase expression was reactivated (34). However those experiments did not address an important question: do the shortened telomeres of senescent cells rescued by telomerase return to normal? If so, does this happen quickly or do the cells need to grow for many cell cycles for telomeres to regain their original lengths?

For this analysis, cells were streaked again and again onto glucose plates until reaching senescence. These cells were harvested and spread onto galactose plates, media conditions that reactivate the *GAL1-V10::EST2* telomerase expression system. As previously observed (34), a large fraction of the senescent cells resumed cycling and formed colonies on the galactose plates. Several colonies from the plates were separately transferred into YPGalactose liquid media and grown overnight at 30 °C in order to recover sufficient amounts of DNA for Southern blot analysis. These cells underwent approximately 20 cell cycles expressing telomerase while growing to form colonies on the galactose plates. After transfer to liquid YPGalactose and overnight growth, the cells divided an additional 10 times, approximately. In total, DNA purified from these cells underwent approximately 30 cell cycles.

Telomere sizes of the (*EST2*) rescued cells remained smaller than normal (See Figure 28, 2nd lane and also Table 2). The sizes listed in Table 2 under Figure 28 represent results for the blot shown in Figure 28. Sizes shown in the final column represent averages from 3 blotting experiments. The average telomere band size for

wildtype cells was 1105 ± 6 bp but was only 1008 ± 21 bp in the cells expressing telomerase for 30 generations.

It is possible that 30 generations is not enough cycles to allow complete replenishment of DNA ends by telomerase. To test this hypothesis, rescued colonies from the initial galactose plates were streaked to new galactose plates, allowed to form colonies over 3 days at 30°C , and then transferred to YPGalactose liquid as before. These cells underwent 30 additional generations (20 on the plate and 10 in the liquid) for a total of 60 generations. Telomere band lengths increased modestly from an average of 1008 ± 21 to 1038 ± 23 bp (Table 2), but remained shorter than wildtype telomeres. Colonies from the 2nd galactose plates were streaked again to new galactose plates and grown in YPGalactose as before. These DNAs experienced 90 generations of growth in the presence of telomerase and telomeres were extended to an average length of 1081 ± 37 bp as shown in Table 2. This size is similar to the average length in wildtype cells, 1105 ± 6 . These results demonstrate that reactivation of telomerase in nondividing late senescent cells restores cell growth potential at a point when telomeres are still quite short. However, if the rescued cells are allowed to grow through enough additional cell cycles, the chromosome ends are restored to approximately normal lengths.

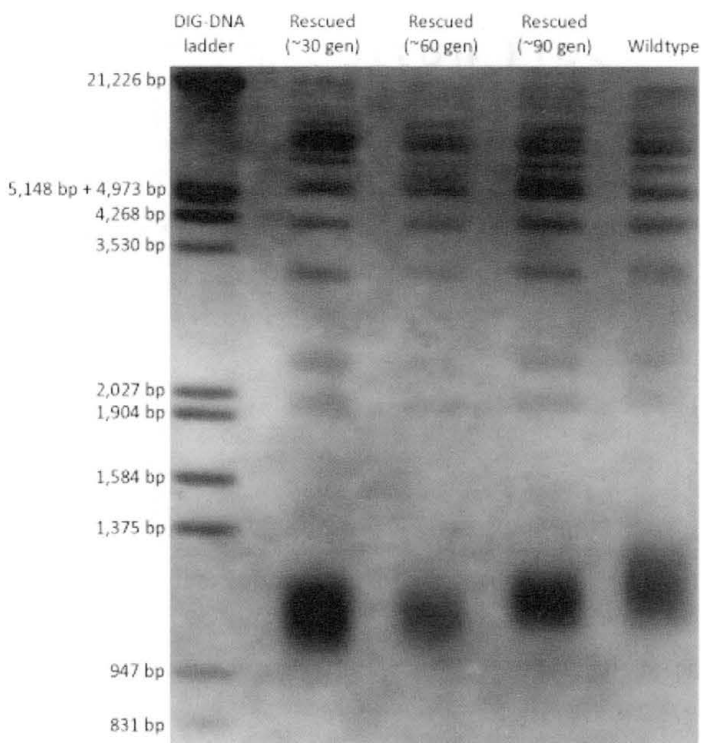


Figure 28. Southern blot analysis of post-senescent telomere length maintenance in YLKL803 cells rescued by (*EST2*) telomerase reactivation.

Table 2. Calculated fragment sizes (bp) of the lower band observed in Southern blots used to evaluate telomere length restoration in telomerase reactivated (*EST2*) cells. Gens, number of generations of growth before DNA was harvested.

Sample	Growth (gens)	Fig. 28 (bp)	Average (bp)
<i>Est2</i> rescued (1 st)	~ 30	985	1008 ± 21 ^a
<i>Est2</i> rescued (2 nd)	~ 60	1019	1038 ± 23 ^a
<i>Est2</i> rescued (3 rd)	~ 90	1051	1081 ± 37 ^a
Wildtype (<i>EST2</i>)	---	1100	1105 ± 6 ^a

^astandard deviation

Summary

The current thesis project involved the development of a new, simplified protocol for purification of yeast chromosomal DNA. As simple eukaryotes, yeasts are a popular model organism and isolating total DNA is routinely performed for many molecular techniques. These cells present particular challenges due to the presence of a rigid cell wall. A commonly used method for disrupting the cells has involved vortexing with small glass beads (38). This form of physical fractionation leads to inadvertent chromosomal shearing, producing smaller DNA fragments (40). The use of lytic enzymes has also been utilized to degrade cell walls. This approach is tedious and can be expensive in large quantities. Another approach involves rapid freeze-thawing to lyse cells followed by extraction using chloroform-phenol (38). This disruption method is also difficult to perform and requires organic solvents. Alternatively, chemical-based methods avert each of these disadvantages and have proven successful for purifying yeast genomic DNA. One drawback is that there are few published chemical-based protocols available. Consequently, dependence remains high on the purchase of expensive commercial products for purification.

One published protocol, the basis of this investigation, involved SDS, an ionic detergent, for cell disruption by solubilizing the lipid components of the cell membrane (40). Various concentrations were tested in the current study and 6% SDS combined with a 65 °C heat shock was deemed optimal based on DNA yield and purity. A separate test revealed that decreasing the duration of the 65 °C heat treatment resulted in decreased lysis efficiency (data not shown). For protein precipitation, potassium acetate solution was found to be superior to sodium acetate. Combining 6% SDS with 30 mM Tris buffer

enhanced DNA yields, though the mechanism involved is unknown. Combining SDS with Tris outperformed SDS alone as well as a commercially available yeast DNA purification kit. Using 3 ml of cells for each purification, the 6% SDS plus Tris method yielded 50 μ l of DNA at a concentration of 200-400 ng/ml. This equates to approximately 15 μ g of total DNA or 5 μ g DNA from each ml of cells, on average. Considering the importance of restriction digestions in molecular biology and genetics research, the DNA purified using the new protocol was tested and confirmed to be a good substrate for restriction enzyme digestion, and also for PCR reactions (data not shown). Furthermore, this protocol is relatively rapid, requiring approximately 1 hour to complete depending on the number of samples.

This thesis project consisted of dual objectives, the second of which expanded upon a previous thesis project conducted in the Lewis laboratory by Sandra Bacerra. That project investigated molecular changes in DNA during eukaryotic cell aging both before and during senescence. A special *Saccharomyces cerevisiae* strain (YLKL803), had been previously engineered to carry out this experiment. The chromosomal copy of *EST2*, encoding the catalytic subunit of the telomerase complex, is deleted from this strain which instead contains the gene on a plasmid vector. Expression is tightly regulated by a galactose inducible promoter, thus allowing telomerase activity to be simply modulated *in vitro* (34).

Wildtype budding yeasts normally express sufficient levels of telomerase to maintain telomere length homeostasis and therefore do not undergo senescence induced by telomere dysfunction (23, 42). Using the telomerase expression system, colonies were repeatedly streaked unto glucose media, suppressing *EST2* expression, to model normal

human aging in somatic cells. Levels of telomere degradation during each streak were quantitated by Southern blot analysis. Results showed that approximately 200 bp of DNA was lost from the chromosome ends by the end of senescence. This amount of loss is significant, considering the reported length of the telomeric DNA tract in *S. cerevisiae* is approximately 350 bp (17, 43).

These data were consistent with the previous project in terms of the estimated number of cell divisions leading to senescence and the levels of telomere shortening. The previous thesis project also demonstrated that most senescent yeast cells that had halted growth could be rescued by reactivating *EST2* expression. Another aim of the current project was to determine if cells rescued from senescence by telomerase reactivation would restore telomere lengths to wildtype levels. Post-senescent cells were allowed to proliferate for 30, 60, and 90 generations with telomerase expressed. Interestingly, average telomere length increased with more generations of growth. Based on the average critically short fragment length attained at the point of senescence (927 bp), 154 bp were restored over the course of 90 generations. The average telomere length after 90 generations, 1081 ± 37 bp, is similar to that of wildtype, which was 1105 ± 6 bp.

Although telomere lengths had undergone significant restoration, 30 and 60 generations of growth expressing telomerase were not a sufficient number of cycles to elongate the chromosome ends to normal lengths. These data indicates that senescent cells that have stopped growing because of shortened telomeres can restore their telomere lengths after reactivation of telomerase. However, approximately 90 generations of growth are required for full restoration. This observation has ramifications for potential future experiments that target telomerase to combat aging in humans and animals.

REFERENCES

1. Zrzepilko, A. *Polish J. Environ. Stud.* **2009**, 18, 399-404.
2. Ohtani, N.; Mann, D.J.; Hara, E. *Cancer Sci.* **2009**, 100, 792-797.
3. Hwang, E.S.; Yoon, G.; Kang, H.T. *Cell. Mol. Life Sci.* **2009**, 66, 2503-2524.
4. Herbig, U.; Ferriera, M.; Condel, L.; Carey, D.; Sedivy, J.M. *Science.* **2006**, 311, 1257.
5. Mathews, C.K.; van Holde, K.E.; Ahern, K.G. *Biochemistry*, 3rd ed; Benjamin Cummings: San Francisco, **2000**.
6. Kotwaliwale, C.V.; Dernburg, A.F. *Cell.* **2009**, 136, 211-212.
7. Watson, J.D.; Baker, T.A.; Bell, S.P.; Gann, A.; Levine, M.; Losick, R. *Molecular Biology of the Gene*, 6th ed. Benjamin Cummings: San Francisco, **2008**.
8. Alberts, B.; Bray, D.; Hopkin, K.; Johnson, A.; Lewis, J.; Raff, M.; Roberts, K.; Walter, P. *Essential Cell Biology*, 2nd ed. Garland Science: New York, **2004**.
9. Dalal, Y.; Furuyama, T.; Vermaak, D.; Henikoff, S. *Proc Natl Acad Sci.* **2007**, 104, 15974-15981.
10. Ahmad, K.; Henikoff, S. *J. Cell Bio.* **2001**, 153, 101-109.
11. Nasmyth, K. *Science.* **2002**, 297, 559-565.
12. Deng, Y.; Chan, S.S.; Chang, S. *Nature.* **2008**, 450-454.
13. Riethman, H.; Ambrosini, A.; Paul, S. *Chromosome. Res.* **2005**, 13, 505-515.
14. Amrane, S.; Lin Ang, R. W.; Tan, Z.M.; Li, C.; Cheow Lim, J.K.; Wen Lim, J.M.; Wai Lim, K.; Phan, A.T. *Nucleic Acids Res.* **2009**, 37, 931-938.
15. Ducray, C.; Pommier, J.P.; Martins, L.; Boussin, F.D.; Sabatier, L. *Oncogene.* **1999**, 18, 4211-4233.

16. Ijpma, A.S.; Greider, C.W. *Mol. Bio Cell.* **2003**, 14, 987-1001.
17. Chen, Y.; Yang, C.; Li, R.; Zeng, R.; Zhou, J. *J. Biol Chem.* **2005**, 280, 24784-24791.
18. Hug, N.; Lingner, J. *Chromosoma.* **2006**, 115, 413-425.
19. Grandin, N.; Damon, C.; Charbonneau, M. *EMBO J.* **2001**, 20, 6127-6139.
20. Russo, I.; Silver, A.; Cuthbert, A.P.; Griffin, D.K.; Trott, D.A.; Newbold, R.F. *Oncogene.* **1998**, 17, 3417-3426.
21. Hackett, J.A.; Greider, C.W. *Mol. Cell. Bio.* **2003**, 23, 8450-8461.
22. LeBel, C.; Welling, R.J. *J. Cell Sci.* **2005**, 118, 2785-2788.
23. Maringele, L.; Lydall, D. *Genes and Dev.* **2004**, 18, 2663-2675.
24. Li, G.Z.; Eller, M.S.; Firoozabadi, R.; Gilchrest, B.A. *PNAS.* **2003**, 100, 527-531.
25. Enomoto, S.; Glowczewski, L.; Lew-Smith, J.; Berman, J.G. *Mol. Cell Bio.* **2004**, 24, 837-845.
26. Itahana, K.; Campisi, J.; Dimri, G.P. *Biogerontology.* **2004**, 5, 1-10.
27. Shawi, M.; Autexier, C. *Mech. Ageing and Development.* **2008**, 129, 3-10.
28. Hackett, J.A.; Greider, C.W. *Oncogene.* **2002**, 21, 619-626.
29. Maniwa, Y.; Yoshimura, M.; Obayashi, C.; Inaba, M.; Kiyooka, K.; Kanki, M.; Okita, Y. *Chest.* **2001**, 120, 589-594.
30. Enomoto, S.; Glowczewski, L.; Berman, J. *Mol. Bio. Cell.* **2002**, 13, 2626-2638.
31. McEachern, M.J.; Iyer, S. *Mol. Cell.* **2001**, 7, 695-704.
32. Ingalls, B.P.; Duncker, B.P.; Kim, D.R.; McConkey, B.J. *Cancer Informatics.* **2007**, 3, 357-370.
33. Hackett, J.A.; Feldser, D.M.; Greider, C.W. *Cell.* **2001**, 106, 275-286.
34. Bacerra, S. *Mechanism of establishment and bypass of in vitro cell aging, Master's Thesis.* **2007**.
35. Narita, M. *British J. Cancer.* **2007**, 96, 686-691.

36. Akada, R.; Murakane, T.; Nishizawa, Y. *Biotechnology*. **2000**, 28, 668-674.
37. Harju, S.; Fedosyuk, H.; Peterson, K.R. *BMC Biotech.* **2004**, 4, 1-6.
38. Kabir, S.; Rajendran, N.; Amemiya, T.; Itoh, K. *J. Biosci and Bioeng.* **2003**, 4, 337-343.
39. Gottschling, D.E.; Singer, M.S. *Science*. **1994**, 266, 404-409.
40. Polaina, J.; Adam, A.C. *Nuc. Acids. Res.* **1991**, 19, 5443.
41. Maser, R.S.; DePinho, R.A. *DNA Repair*. **2004**, 3, 979-988.
42. Blackburn, E.H. *Cell*. **2001**, 106, 661-673.
43. Lunblad, V. Budding Yeast Telomeres. *Telomeres*, 2nd ed.; CSH Press: New York, **2006**; 345-386.

VITA

Christopher Keith Lee was born in Alexandria, Louisiana on July 30, 1981, the son of Keith Lee and Sharen K. Lee. After graduating from Many High School, Many, Louisiana, in 2000, he enrolled at Northwestern State University in historic Natchitoches, Louisiana. He was a 2-year member of the university rowing club and competed in the prestigious Dad Vail Regatta in Philadelphia. He received the degree of Bachelor of Science in biology with a chemistry minor in May 2005. In August 2007, he entered the Graduate College of Texas State University-San Marcos. In October of 2009, he was hired by Biomat USA (Austin, TX) and began a professional career in science.

Permanent Address: 1228 San Antonio Ave

Many, Louisiana 71449

This thesis was typed by Christopher Keith Lee